UNIVERSITY OF CALIFORNIA, MERCED

MASTER'S THESIS

Modeling the time evolution of tide level, salinity, temperature, and oxygen concentration in marine lakes, Palau

by

Sydney Montroy

A technical report submitted
in partial fulfillment of the requirements for the degree of

Master of Science in Applied Mathematics

2013

Committee Members:
Professor François Blanchette, Chair
Professor Mike Dawson
Professor Karin Leiderman

UNIVERSITY OF CALIFORNIA, MERCED
Graduate Division

This is to certify that I have examined a copy of a technical report by

Sydney Montroy

and found it satisfactory in all respects, and that any and all revisions required by the examining committee have been made.

Applied Mathematics
Graduate Studies Chair:

_____
Professor Boaz Ilan

Thesis Committee:

_____
Professor Mike Dawson

Thesis Committee:

_____
Professor Karin Leiderman

Committee Chair / Research Advisor:

_____
Professor François Blanchette

_____
Date

Acknowledgements

I would first like to thank Professor Karin Leiderman for all of the constructive criticism and feedback she contributed to my thesis.

Thank you to Professor Mike Dawson for all of the data and biological expertise he provided throughout the process.

I would also like to thank Andrew Regopoulos for the unwavering support and confidence he gave me all throughout graduate school.

Last but certainly not least, I would like to thank Professor François Blanchette. This endeavor would not have been possible without his dedicated help, invaluable guidance, and constant encouragement. From the time that I was an undergraduate student, he went above and beyond what was required of him to push me beyond my perceived limits. His advice has been invaluable to me both in and out of school and I continue to look forward to where it will lead me in the future. Thank you for never losing sight of my capabilities.

Contents

Modeling the time evolution of tide level, salinity, temperature, and oxygen concentration in marine lakes, Palau

by

Sydney Montroy

Master of Science in Applied Mathematics

Professor François Blanchette, Chair

University of California, Merced

2013

Abstract

We aim to model the time evolution of the tide level, salinity, temperature, and oxygen content of a marine lake. We focus on the marine lake in Palau called Ongeim'l Tketau, for which we have detailed physical limnological data. By modeling the concentrations of water flowing through the underground tunnels, which connect the lake to the surrounding ocean, we are able to achieve stable lake concentration conditions over time. The model includes a wide array of parameters that can be varied to explore different climate and initial conditions. We are successful at modeling the salinity profile in the lake during a tropical storm. This model could be used to explore a marine lake's response to natural mixing, human caused effects, and changes in climate.

List of Symbols

- $A(z)$: Area of lake at a given height z (length^2)
- $cr(z)$: Density of influx of rain water in lake $\left(\frac{1}{\text{length}}\right)$
- $D_e(z,t)$: Coefficient of effective mixing $\left(\frac{\text{length}^2}{\text{time}}\right)$
- $\hat{d}(z)$: Integrated distribution function of water entering or exiting lake $\left(\frac{1}{\text{length}}\right)$
- $Ev(t)$: Evaporation rate at surface of lake $\left(\frac{\text{length}}{\text{time}}\right)$
- $L(t)$: Deviation of lake level from its mean over one tidal cycle (length)
- $O(t)$: Deviation of ocean level from its mean over one tidal cycle (length)
- $Oc(z,t)$: Oxygen consumption of lake $\left(\frac{\text{mass}}{\text{length}^3\text{time}}\right)$
- $Os(t)$: Salinity of ocean water $\left(\frac{\text{mass}}{\text{length}^3}\right)$
- $\overline{Ox}(z,t)$: Horizontally averaged concentration of oxygen in lake $\left(\frac{\text{mass}}{\text{length}^3}\right)$
- $Oxr(t)$: Oxygen content of rain $\left(\frac{\text{mass}}{\text{length}^3}\right)$
- $R(t)$: Rate of rainfall $\left(\frac{\text{length}}{\text{time}}\right)$
- $S(A(z),z,t)$: Concentration of salt in lake $\left(\frac{\text{mass}}{\text{length}^3}\right)$
- $\bar{S}(z,t)$: Horizontally averaged concentration of salt in lake $\left(\frac{\text{mass}}{\text{length}^3}\right)$
- $SH(z,t)$: Solar heat rate in lake $\left(\frac{^\circ\text{C}}{\text{time}}\right)$
- $Sr(t)$: Salinity of rainwater $\left(\frac{\text{mass}}{\text{length}^3}\right)$
- $St(x,z,t)$: Salinity of water in tunnels $\left(\frac{\text{mass}}{\text{length}^3}\right)$
- t : Time
- $\bar{T}(z,t)$: Horizontally averaged temperature of lake (°C)
- $Tr(t)$: Temperature of rainwater (°C)
- $Tu(z)$: Average location of transport connections between the lake and ocean (1)

- $u(z,t)$: Vertical velocity of lake water $\left(\frac{\text{length}}{\text{time}}\right)$
- $u_{\text{tunnel}}(z,t)$: Horizontal velocity of water in tunnels $\left(\frac{\text{length}}{\text{time}}\right)$
- ω : Proportionality constant that represents the rate given by the ratio of pressure difference between the lake and ocean multiplied by the permeability and divided by the viscosity (Darcy's Law) $\left(\frac{1}{\text{time}}\right)$

List of Figures

1 Introduction

Palau is an island country in the Pacific Ocean that has a tropical climate and receives heavy rainfall throughout the year. On many of its smaller islands, there exist saline lakes that are connected to the ocean by underground tunnels [1]. As with other lakes, the dynamics of these tropical saline lakes are subject to the effects of solar heat [2]; these lakes are also influenced by tropical storms and changes in ocean characteristics. Some of these lakes are inhabited by large populations of $Mastigias\ papua$, or 'golden jellyfish' that can cause additional mixing in the lake [3]. In this paper, we aim to model the level, salinity, temperature, and oxygen content of a marine lake based on the ocean level, initial lake conditions, and weather.

Professor Mike Dawson and his lab in U.C. Merced's Quantitative and Systems Biology graduate group, and the Coral Reef Research Foundation, have collected data over a span of several years on one particular lake called Ongeim'l Tketau (Jellyfish Lake) [4]. Using this information, we have developed a mathematical model that simulates the salinity, temperature, and oxygen concentration in the lake over time. We make the model two-dimensional by averaging each concentration over the area of the lake for a given depth. By incorporating many different adjustable parameters, we make the model complex enough to be able to explore responses to a tropical storm. We also refined the model to simulate how these concentrations change in the underground tunnels so that we can more accurately determine the water concentrations that are entering the lake from the ocean. This is a key component to the model since it takes into account the travel distance and possible changes in concentrations that occur as water flows between the lake and the ocean.

Our purpose in creating this model is to understand how changes in weather and climate affect the dynamics of marine lakes. The model takes into account the fact that the properties of the water traveling from the ocean to the lake may change before it reaches the lake. It also provides the flexibility to simulate many different scenarios through the ability to adjust a wide array of parameters. Both of these factors will allow for the model to be used to investigate how external changes can affect the lake and its ecosystem over a given period of time. In the subsequent sections, we will develop methods to model the tide level and concentrations of a marine lake as well as the concentrations of water in underground tunnels between the lake and ocean. Later we will compare our tunnel model with actual data and present the results of a storm simulation.

2 Derivation of Governing Equations

2.1 Lake Level

We begin by deriving the equation governing the level of the lake, $L(t)$. We will make the assumption that the average vertical velocity of lake water is independent of fluid properties. In other words, there is no large scale vertical motion due to differences in concentrations, such as salinity or temperature. We also assume that the mass flux of the lake is proportional to the surface density difference between the lake and the ocean. We neglect both the contribution of rainfall and evaporation to the lake level since they are of order 10^{-5} [5] and 10^{-6} [6] m/min, respectively, while the order of $\frac{dL}{dt}$ is 10^{-3} m/min. With these assumptions, we arrive at the following equation for the level of the lake:

$$\frac{dL}{dt} = \omega \left(\frac{\rho_O}{\rho_L} O(t) - L(t) \right), \tag{1}$$

where $O(t)$ represents the level of the ocean. Equation (1) represents the vertical velocity of the lake surface, taking into account the density variation between the ocean and the lake, ρ_O/ρ_L. The proportionality constant, ω, is related to the porosity of the medium between the lake and ocean and has units of $\frac{1}{\text{time}}$. We choose to use this fairly simply differential equation to determine the lake level due to the fact that we do not have a good idea of the value of the permeability of medium between ocean and lake that would allow for a more complex model. Additionally, it is worth noting that a more complex model may or may not better approximate the lake level. We will later approximate the value of this constant by matching the lake level obtained from the model with actual lake level data.

2.2 Salinity Equation

To track the salinity, temperature, and oxygen content in the lake, we set up the vertical z-axis such that $z = 0$ corresponds to the mean lake surface level over one tidal cycle and z increases with depth. The three concentrations that we are modeling, salinity, $\bar{S}$, temperature, $\bar{T}$, and oxygen, $\overline{Ox}$, are governed by very similar equations. We start by deriving the equation for salinity and then discuss the differences that exist between the other two equations.

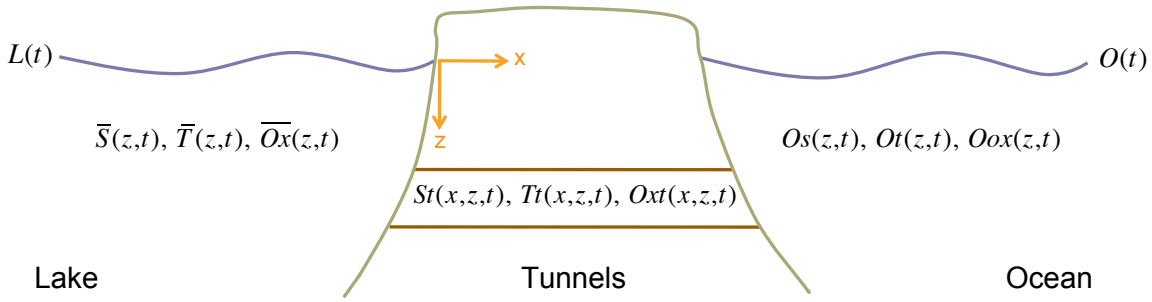

Figure 1: Set up for concentration tracking model.

We first define $S(A(z), z, t)$ as the concentration of salt in the lake as a function of the horizontal area of the lake, $A(z)$, at some depth z. We use the notation $\bar{S}(z,t)$ (see Figure 1) for the salinity of lake water averaged over the area of a slice,

$$\bar{S}(z,t) = \frac{1}{A(z)} \iint_{A(z)} S(A(z), z, t) dA,$$

and $M(z,t)$ as the mass of salt per unit thickness, Δz, of a slice. Consequently, $M(z,t)\Delta z$ represents the mass of salt in a slice. We define $D_e(z,t)$ to be the diffusion coefficient of lake water and $Q(z,t)$ as any horizontally averaged source/sink terms. Performing a mass balance (see Figure 2) over a slice yields the following equations:

$$M(z, t+\Delta t)\Delta z = M(z,t)\Delta z + \Delta t D_e(z+\Delta z, t) \iint_{A(z+\Delta z)} \frac{\partial S(A(z), z, t)}{\partial z} dA$$
$$- \Delta t D_e(z,t) \iint_{A(z)} \frac{\partial S(A(z), z, t)}{\partial z} dA + Q(z,t),$$

$$A(z)\left(\frac{\bar{S}(z, t+\Delta t) - \bar{S}(z,t)}{\Delta t}\right) =$$
$$\frac{D_e(z+\Delta z+\Delta z, t) \iint_{A(z+\Delta z)} \frac{\partial S(A(z),z,t)}{\partial z} dA - D_e(z,t) \iint_{A(z)} \frac{\partial S(A(z),z,t)}{\partial z} dA}{\Delta z} + Q(z,t).$$

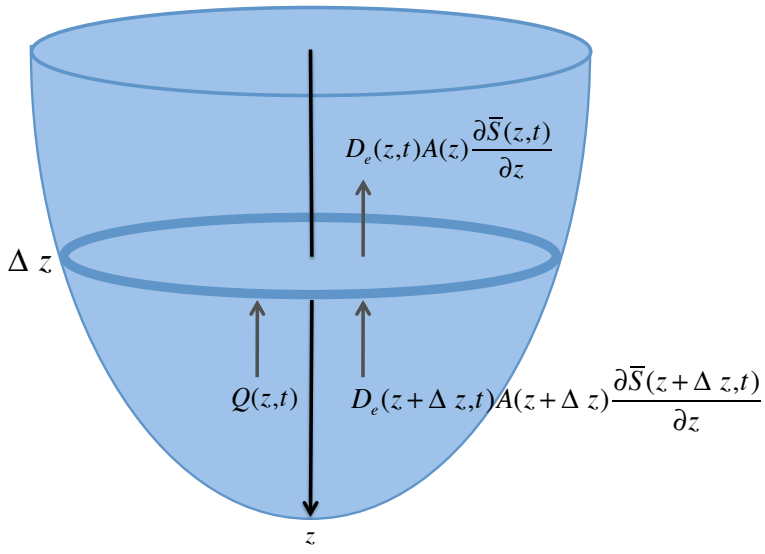

Figure 2: Mass balance schematic for diffusion term.

Taking the limit as $\Delta z \to 0$ and $\Delta t \to 0$ yields

$$A(z)\frac{\partial \bar{S}(z,t)}{\partial t} = \frac{\partial}{\partial z}\left(D_e(z,t)\iint_{A(z)}\frac{\partial S(A(z),z,t)}{\partial z}dA\right) + Q(z,t). \tag{2}$$

To put the diffusion component in terms of $\bar{S}(z,t)$, we first use the Leibniz integral rule to compute:

$$\iint_{A(z)}\frac{\partial S(A(z),z,t)}{\partial z}dA.$$

This gives us the following:

$$\frac{\partial}{\partial z}\left(\iint_{A(z)}\frac{\partial S(z,t)}{\partial z}dA\right) = \int_{\partial A(z)}\frac{\partial A(z)}{\partial z}S(\partial A(z),z,t)ds + \iint_{A(z)}\frac{\partial S(A(z),z,t)}{\partial z}dA,$$

$$\iint_{A(z)}\frac{\partial S(A(z),z,t)}{\partial z}dA = \frac{\partial}{\partial z}(A(z)\bar{S}(z,t)) - \frac{\partial A}{\partial z}\int_{\partial A(z)}S(\partial A(z),z,t)ds,$$

$$\iint_{A(z)}\frac{\partial S(A(z),z,t)}{\partial z}dA = \frac{\partial A}{\partial z}\bar{S}(z,t) + A(z)\frac{\partial \bar{S}}{\partial z} - \frac{\partial A}{\partial z}\int_{\partial A(z)}S(\partial A(z),z,t)ds. \tag{3}$$

At this point, we will make the assumption that $\bar{S}(z,t) \approx \int_{\partial A(z)} S(\partial A(z), z, t) ds$ because we do not have any better information that would allow us to make any other assumption. In other words, the average salinity at height z is approximately equal to the average salinity around the boundary at the same height z. Applying this assumption to equation (3) yields the following:

$$\iint_{A(z)} \frac{\partial S(A(z), z, t)}{\partial z} dA = A(z) \frac{\partial \bar{S}}{\partial z}.$$

Equation (2) becomes

$$A(z) \frac{\partial \bar{S}(z,t)}{\partial t} = \frac{\partial}{\partial z} \left(D_e(z,t) A(z) \frac{\partial \bar{S}(z,t)}{\partial z} \right) + Q(z,t). \tag{4}$$

Now we will describe the integrated sources and sinks for when water is exiting and entering the lake. We define $u(z,t)$ as the vertical velocity of lake water and $v(z,t)$ as the volume flow rate of lake water out of the side of the lake at depth z. Performing a volume flow rate balance over a slice yields the following relation:

$$\begin{aligned} u(z+\Delta z, t) A(z+\Delta z) &= u(z,t) A(z) - v(z,t), \\ \frac{u(z+\Delta z, t) A(z+\Delta z) - u(z,t) A(z)}{\Delta z} &= -\frac{v(z,t)}{\Delta z}, \\ \frac{\partial}{\partial z} \left(u(z,t) A(z) \right) &= -\lim_{\Delta z \to 0} \left(\frac{v(z,t)}{\Delta z} \right). \end{aligned}$$

To determine the conditions under which the limit in the equation above is finite as $\Delta z \to 0$, we further define $v(z,t)$ as the product of the horizontal velocity of water flowing out of the lake, $w(z,t)$, and the surface area of the walls of the lake, $SA(z)$, at depth z. We determine the equation for the surface area to be:

$$SA(z) = P(z)\, \Delta z \sqrt{\left(\frac{r(z) - r(z+\Delta z)}{\Delta z} \right)^2 + 1},$$

where $P(z)$ represents the average perimeter of a slice and $r(z)$ is the average radius of the lake at a given depth. Now taking the limit as $\Delta z \to 0$:

$$\lim_{\Delta z \to 0} \left(\frac{v(z,t)}{\Delta z} \right) = \lim_{\Delta z \to 0} \left(\frac{w(z,t) P(z) \Delta z \sqrt{\left(\frac{r(z) - r(z+\Delta z)}{\Delta z} \right)^2 + 1}}{\Delta z} \right)$$
$$= w(z,t)\, P(z) \sqrt{\left(\frac{dr}{dz} \right)^2 + 1}.$$

Since we have data available for $A(z)$ and not $r(z)$ [5], we rewrite the equation above in terms of $A(z)$. With the assumption that $A(z) = C_1 r(z)^2$, where C_1 is a constant, we find that

$$\lim_{\Delta z \to 0} \left(\frac{v(z,t)}{\Delta z} \right) = w(z,t)\, P(z) \sqrt{\frac{C_0}{A(z)} \left(\frac{dA}{dz} \right)^2 + 1},$$

where C_0 is some constant. This limit is finite under the following condition:

$$\left| \frac{1}{A(z)} \left(\frac{dA}{dz} \right)^2 \right| \leq M,$$

where M is a finite number.

Next we define a volume flow distribution function, $Tu_{out}(z)$, of outgoing lake water that has the following property:

$$\int_{-\infty}^{\infty} Tu_{out}(z) dz = 1.$$

Figure 3 shows a typical choice of Tu_{out}. Each peak corresponds to the depth of a known tunnel, where the inflow is therefore enhanced.

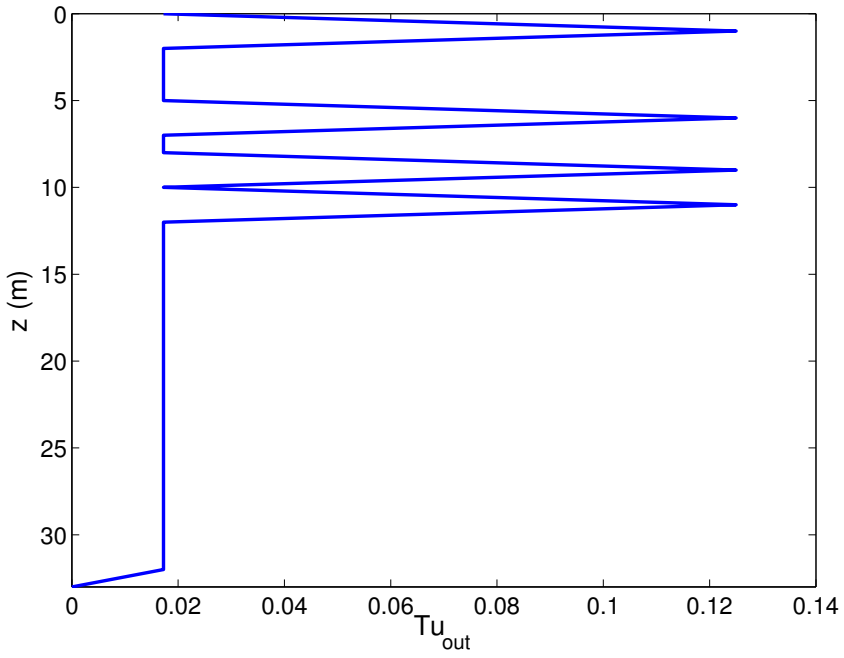

Figure 3: Distribution of outflow of water from lake.

This enables us to define the volume flow rate of lake water at a given depth to be

$$u(z,t)A(z) = u(0,t)A(0)\int_{-\infty}^{z} Tu_{out}(z')dz'. \tag{5}$$

Note that since $u(0,t)$ is the vertical velocity of the surface of the lake, it satisfies $u(0,t) = -\frac{dL}{dt}$. Now we can perform a mass balance over a slice yielding the advection term in the scenario where water is exiting the lake (see Figure 4):

$$\begin{aligned} M(z,t+\Delta t)\Delta z = {} & M(z,t)\Delta z + u(z,t)M(z,t)\Delta t \\ & - u(z+\Delta z,t)M(z+\Delta z,t)\Delta t - v(z,t)\bar{S}(z,t)\Delta t, \end{aligned}$$

$$\begin{aligned} & \frac{A(z)\bar{S}(z,t+\Delta t) - A(z)\bar{S}(z,t)}{\Delta t} = \\ & -\left(\frac{u(z+\Delta z,t)A(z+\Delta z)\bar{S}(z+\Delta z,t) - u(z,t)A(z)\bar{S}(z,t)}{\Delta z}\right) - \frac{v(z,t)}{\Delta z}\bar{S}(z,t), \end{aligned}$$

$$\frac{\partial}{\partial t}(A(z)\bar{S}(z,t)) = -\frac{\partial}{\partial z}(u(z,t)A(z)\bar{S}(z,t)) + \frac{\partial}{\partial z}(u(z,t)A(z))\bar{S}(z,t), \tag{6}$$

$$A(z)\frac{\partial \bar{S}(z,t)}{\partial t} = -u(z,t)A(z)\frac{\partial \bar{S}(z,t)}{\partial z},$$

$$A(z)\frac{\partial \bar{S}(z,t)}{\partial t} = -u(0,t)A(0)\int_{-\infty}^{z} Tu_{out}(z')dz'\frac{\partial \bar{S}(z,t)}{\partial z}.$$

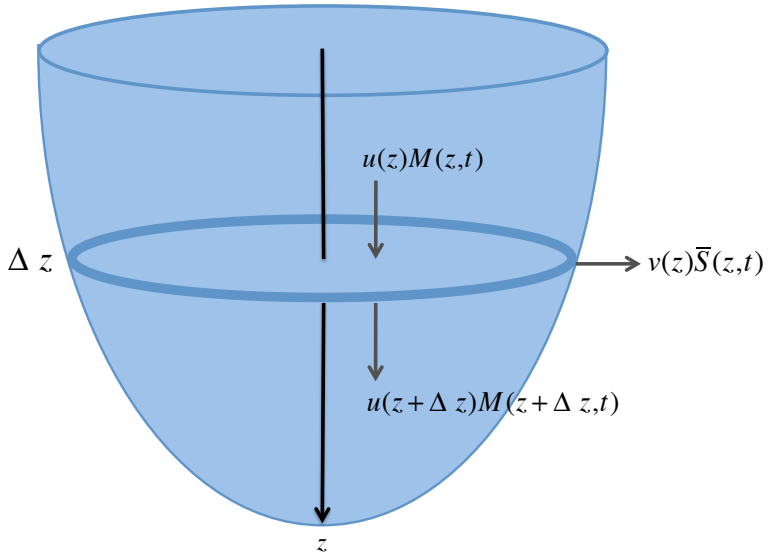

Figure 4: Mass balance schematic for advection outflow term.

Similarly, we perform a volume flow rate balance over a slice to derive the incoming advection of salt:

$$\begin{aligned} -u(z+\Delta z,t)A(z+\Delta z) + v(z,t) &= -u(z,t)A(z), \\ \frac{u(z+\Delta z,t)A(z+\Delta z) - u(z,t)A(z)}{\Delta z} &= \frac{v(z,t)}{\Delta z}, \\ \frac{\partial}{\partial z}(u(z,t)A(z)) &= \lim_{\Delta z \to 0}\left(\frac{v(z,t)}{\Delta z}\right). \end{aligned}$$

The volume flow rate distribution function of incoming water, $Tu_{in}(z)$, is defined in the same way as $Tu_{out}(z)$, though the two functions need not be the same. As before, we can perform a mass balance over a slice, yielding the advection term in the scenario where

water is entering the lake:

$$M(z,t+\Delta t)\Delta z = M(z,t)\Delta z - u(z+\Delta z,t)M(z+\Delta z,t)\Delta t + u(z,t)M(z,t)\Delta t + v(z,t)Os(z,t)\Delta t,$$

$$\frac{A(z)\bar{S}(z,t+\Delta t) - A(z)\bar{S}(z,t)}{\Delta t} = -\left(\frac{u(z+\Delta z,t)A(z+\Delta z)\bar{S}(z+\Delta z,t) - u(z,t)A(z)\bar{S}(z,t)}{\Delta z}\right) + \frac{v(z,t)}{\Delta z}Os(z,t),$$

$$\frac{\partial}{\partial t}(A(z)\bar{S}(z,t)) = -\frac{\partial}{\partial z}\left(u(z,t)A(z)\bar{S}(z,t)\right) + \frac{\partial}{\partial z}\left(u(z,t)A(z)\right)Os(z,t), \tag{7}$$

$$A(z)\frac{\partial \bar{S}(z,t)}{\partial t} = \frac{\partial}{\partial z}\left(u(z,t)A(z)(Os(z,t) - \bar{S}(z,t))\right) - u(z,t)A(z)\frac{\partial Os(z,t)}{\partial z},$$

$$A(z)\frac{\partial \bar{S}(z,t)}{\partial t} = u(0,t)A(0)\left(\frac{\partial}{\partial z}\left((\bar{S}(z,t) - Os(z,t))\int_{-\infty}^{z} Tu_{in}(z')dz'\right) - \frac{\partial Os(z,t)}{\partial z}\int_{-\infty}^{z} Tu_{in}(z')dz'\right).$$

At this point we observe that equations (6) and (7) are the same except for the second salinity term. If we replace the salt concentration term with a general salt concentration $\hat{S}(z,t)$, and velocity with a general velocity, $\hat{u}(z,t)$, we get the following equations:

$$A(z)\frac{\partial \bar{S}(z,t)}{\partial t} = -\frac{\partial}{\partial z}\left(\hat{u}(z,t)A(z)\bar{S}(z,t)\right) + \frac{\partial}{\partial z}(\hat{u}(z,t)A(z))\hat{S}(z,t),$$

$$A(z)\frac{\partial \bar{S}(z,t)}{\partial t} = \frac{\partial}{\partial z}\left(\hat{u}(z,t)A(z)(\hat{S}(z,t) - \bar{S}(z,t))\right) - \hat{u}(z,t)A(z)\frac{\partial \hat{S}(z,t)}{\partial z}.$$

Now we can plug in equation (5) using a general function $\hat{d}(z)$ in place of the incoming or outgoing integrated volume flow rate distribution function:

$$A(z)\frac{\partial \bar{S}(z,t)}{\partial t} = \frac{\partial}{\partial z}\left(u(0,t)A(0)\hat{d}(z)(\hat{S}(z,t) - \bar{S}(z,t))\right) - u(0,t)A(0)\hat{d}(z)\frac{\partial \hat{S}(z,t)}{\partial z},$$

$$A(z)\frac{\partial \bar{S}(z,t)}{\partial t} = u(0,t)A(0)\left(\frac{\partial}{\partial z}\left(\hat{d}(z)(\hat{S}(z,t) - \bar{S}(z,t))\right) - \hat{d}(z)\frac{\partial \hat{S}(z,t)}{\partial z}\right),$$

where

$$\hat{d}(z) = \begin{cases} \int_{-\infty}^{z} Tu_{in}(z')dz' & \text{if } \frac{dL}{dt} > 0 \\ \\ \int_{-\infty}^{z} Tu_{out}(z')dz' & \text{if } \frac{dL}{dt} < 0 \end{cases}$$

and

$$\hat{S}(z,t) = \begin{cases} St(0,z,t) & \text{if } \frac{dL}{dt} > 0 \\ \\ \bar{S}(z,t) & \text{if } \frac{dL}{dt} < 0. \end{cases}$$

The above form takes both incoming and outgoing advective terms into account with their respective salinity, $\hat{S}(z,t)$, and distribution function, $\hat{d}(z)$. $St(0,z,t)$ is defined as the salinity of water in a tunnel or in the porous medium between the lake and ocean when it reaches the lake.

The last component remaining in the salinity equation is the source term due to rainfall. We define $cr(z)$ to be the density of influx of rain water in the lake, which integrates to 1 over the entire depth of the lake. A typical choice of $cr(z)$ is shown in Figure 5.

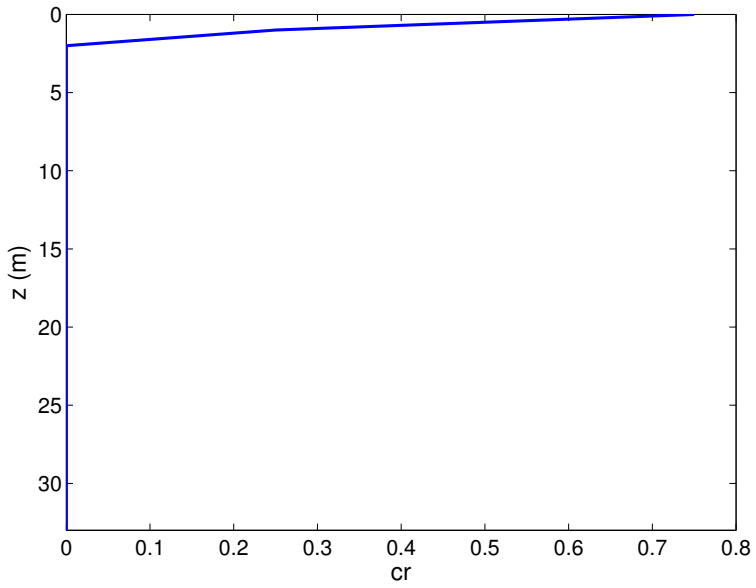

Figure 5: Distribution of inflow of rainwater in lake.

Following from this definition, we can derive the rain source term as follows:

$$A(0)R(t)cr(z)(Sr(t) - \bar{S}(z,t)),$$

where $R(t)$ is the rate of rainfall and $Sr(t)$ is the salinity of rain. Putting everything together, we arrive at our final salinity equation:

$$\begin{aligned} A(z)\frac{\partial \bar{S}(z,t)}{\partial t} = & \frac{\partial}{\partial z}\left(D_e(z,t)A(z)\frac{\partial \bar{S}(z,t)}{\partial z}\right) \\ & + u(0,t)A(0)\left(\frac{\partial}{\partial z}\left(\hat{d}(z)(\hat{S}(z,t) - \bar{S}(z,t))\right) - \hat{d}(z)\frac{\partial \hat{S}(z,t)}{\partial z}\right) \\ & + A(0)R(t)cr(z)(Sr(t) - \bar{S}(z,t)). \end{aligned} \tag{8}$$

Now that we have finished deriving the salinity equation, we examine the boundary conditions at $z = 0$ and $z = N$, where N is the depth of the lake. To derive our boundary conditions, we start with the basic advection-diffusion equation,

$$A(z)\frac{\partial \bar{S}(z,t)}{\partial t} = \frac{\partial}{\partial z}\left(A(z)D_e(z,t)\frac{\partial \bar{S}(z,t)}{\partial z}\right) - \frac{\partial}{\partial z}\left(A(z)u(z,t)\bar{S}(z,t)\right).$$

The integral of this equation over the entire depth of the lake is equivalent to the time

derivative of the mass of salt in the lake. We assume that there is no inflow or outflow of salt, so it is equal to zero. Using the Leibniz integral rule, we integrate the equation over the entire depth of the lake, taking into account the moving boundary:

$$\begin{aligned}
0 =& \frac{\partial}{\partial t}\int_{G(t)}^{0} A(z')\bar{S}(z',t)dz', \\
0 =& -\frac{\partial L}{\partial t}A(G(t))\bar{S}(G(t),t) + \int_{G(t)}^{0}\frac{\partial}{\partial z'}\left(A(z')D_e(z',t)\frac{\partial \bar{S}(z',t)}{\partial z'}\right) \\
& - \frac{\partial}{\partial z'}\left(A(z')u(z',t)\bar{S}(z',t)\right)dz',
\end{aligned}$$

$$\begin{aligned}
0 =& -u(G(t),t)A(G(t))\bar{S}(G(t),t) + A(0)D_e(0,t)\frac{\partial \bar{S}(0,t)}{\partial z'} \\
& - A(G(t))D_e(G(t),t)\frac{\partial \bar{S}(G(t),t)}{\partial z'} - A(0)u(0,t)\bar{S}(0,t) \\
& + A(G(t))u(G(t),t)\bar{S}(G(t),t),
\end{aligned}$$

$$0 = A(0)D_e(0,t)\frac{\partial \bar{S}(0,t)}{\partial z'} - A(G(t))D_e(G(t),t)\frac{\partial \bar{S}(G(t),t)}{\partial z'} - A(0)u(0,t)\bar{S}(0,t).$$

Note that here the vertical z-axis is oriented so that it increases in the upward direction. This is for the purpose of being consistent with how we track the level of the lake, $L(t)$. We define $G(t)$ to be the level of the lake, where $G(t) = N + L(t)$. Since the velocity at the bottom of the lake is zero ($u(0,t) = 0$), we can simplify the equation:

$$0 = A(0)D_e(0,t)\frac{\partial \bar{S}(0,t)}{\partial z'} - A(G(t))D_e(G(t),t)\frac{\partial \bar{S}(G(t),t)}{\partial z'}.$$

Assuming the boundary conditions at the top and bottom of the lake are independent, to derive the boundary condition at the top, we temporarily assume that there is no flux of salt at the bottom of the lake. We write these boundary conditions to be consistent with the axis set up for the salinity concentration model. This yields zero Neumann boundary conditions at the top of the lake:

$$A(z)D_e(z,t)\frac{\partial \bar{S}}{\partial z}\bigg|_{z=0} = 0 \qquad \rightarrow \qquad \frac{\partial \bar{S}}{\partial z}\bigg|_{z=0} = 0.$$

Similarly at the bottom of the lake, we temporarily assume that there is no flux at the top of the lake, yielding zero Neumann boundary conditions at the bottom of the lake:

$$A(z)D_e(z,t)\frac{\partial \bar{S}}{\partial z}\bigg|_{z=N} = 0 \qquad \rightarrow \qquad \frac{\partial \bar{S}}{\partial z}\bigg|_{z=N} = 0.$$

2.3 Temperature and Oxygen Equations

Now that we have completed the derivation of the salinity equation and its associated boundary conditions, we discuss the differences that exist between this boundary value problem and that for temperature and oxygen. All three of these quantities are governed by very similar equations since their dynamics are determined by fluid flow. The advection, diffusion, and rain terms are the same for each concentration since they are all carried by the same fluid. Beginning with the temperature equation, the governing equation is the same as that for salinity, other than an additional source term for solar heat:

$$\begin{aligned} A(z)\frac{\partial \bar{T}(z,t)}{\partial t} &= \frac{\partial}{\partial z}\left(D_e(z,t)A(z)\frac{\partial \bar{T}(z,t)}{\partial z}\right) \\ &\quad + u(0,t)A(0)\left(\frac{\partial}{\partial z}\left(\hat{d}(z)(\hat{T}(z,t)-\bar{T}(z,t))\right) - \hat{d}(z)\frac{\partial \hat{T}(z,t)}{\partial z}\right) \\ &\quad + A(0)R(t)cr(z)(Tr(t)-\bar{T}(z,t)) + \underline{A(z)Sh(z,t)}. \end{aligned} \tag{9}$$

$Tr(t)$ is defined as the temperature of rainwater and $Sh(z,t)$ is a temperature rate due to heat from the sun that decays exponentially from the surface of the lake. The boundary conditions for temperature also differ from those for salinity. Instead of zero Neumann boundary conditions, we use non-homogeneous Dirichlet boundary conditions:

$$\bar{T}(0,t) = T_{\text{air}}(t), \qquad \bar{T}(N,t) = T_{\text{rock}}(t).$$

Although the top boundary condition could be made more complex to include effects due to wind or evaporation, we use this form for the time being for the purpose of simplicity.

The governing equation for oxygen is very similar to that for temperature, except that the additional sink term is due to oxygen consumption in the lake:

$$\begin{aligned} A(z)\frac{\partial \overline{Ox}(z,t)}{\partial t} &= \frac{\partial}{\partial z}\left(D_e(z,t)A(z)\frac{\partial \overline{Ox}(z,t)}{\partial z}\right) \\ &\quad + u(0,t)A(0)\left(\frac{\partial}{\partial z}\left(\hat{d}(z)(\widehat{Ox}(z,t)-\overline{Ox}(z,t))\right) - \hat{d}(z)\frac{\partial \widehat{Ox}(z,t)}{\partial z}\right) \\ &\quad + A(0)R(t)cr(z)(Oxr(t)-\overline{Ox}(z,t)) - \underline{A(z)Oc(z,t)}, \end{aligned} \tag{10}$$

where $Oc(z,t)$ is the rate of oxygen consumption in the lake. This consumption rate de-

pends primarily on microorganisms not modeled in this paper and would typically scale like a population of microorganisms. The boundary condition at the bottom of the lake is that same as that for salinity, i.e. there is no flux of oxygen at the bottom of the lake. For lack of better information to make the top boundary condition more complex, we use a non-homogeneous Dirichlet boundary condition at the top of the lake. The boundary conditions for oxygen content in the lake are as follows:

$$\overline{Ox}(0,t) = Ox_{\max}, \qquad \left.\frac{\partial \overline{Ox}}{\partial z}\right|_{z=N} = 0,$$

where $Ox_{\max}$ is defined as the maximum oxygen content in the lake.

2.4 Tunnel Concentrations

To model the salinity, temperature, and oxygen content of water flowing through the tunnels, we set up a horizontal x-axis such that $x = 0$ corresponds to where the tunnel meets the lake and the value of x increases as one moves away from the lake (see Figure 1). We use this model to not only track the concentration of water entering the lake from a tunnel, but also at any other depth in the lake without a tunnel. The difference between tunnel flow and seepage being that the horizontal velocity of water flowing into the lake at a depth without a tunnel will be significantly less than at a depth with a tunnel. All three concentrations are governed by the same equation as they are carried by the same flow. As water flows through a tunnel, each concentration can change due to advection and any source or sink effect through the walls of the tunnel. We describe the equation for salinity as an example:

$$\frac{\partial St(x,z,t)}{\partial t} + u_{\text{tunnel}}(z,t)\frac{\partial St(x,z,t)}{\partial x} = -\alpha St(x,z,t). \tag{11}$$

In the equation above, we define $u_{\text{tunnel}}(z,t)$ as the horizontal velocity of water in a tunnel. Since we only have data [5] available for the velocity of water at the mouth of the tunnel and not inside the tunnel, we make the assumption that the velocity of water in each tunnel does not change with respect to x. α is defined as the rate at which the concentration is gained or lost through the walls of the tunnel. For instance, if the walls of the tunnel are much colder than the water flowing from the ocean, the temperature of the water may decrease as it flows toward the lake. However, since we do not have any data that we could use to get a good approximation of α for any concentration, we assume that this parameter is zero, meaning that no concentration is being gained or lost through the walls of a tunnel.

We obtain an exact solution to equation (11) of the form

$$St(x,z,t) = f\left(x - \int_0^t u_{\text{tunnel}}(z,t')dt'\right),$$

where

$$f(\eta) = \begin{cases} c_1(Os(z,t) - \bar{S}(z,t))(\eta - \eta_0) + \bar{S}(z,t) & \text{if} \quad 0 < \eta < D \\ c_2(\bar{S}_{\max}(z,t) - \bar{S}(z,t))(\eta - \eta_{\max}) + \bar{S}_{\max}(z,t) & \text{if} \quad -d < \eta < 0 \\ \bar{S}(z,t) & \text{if} \quad \eta < -d. \end{cases}$$

$\bar{S}_{\max}(z,t)$ is defined to be the maximum value that the salinity reaches at the mouth of the tunnel and η_0 and $\eta_{\max}$ depend on the when the tide changes direction. Although D is defined as the length of the tunnel and d is the horizontal distance over which tunnel water flows into the lake, in practice, these parameters are not needed in the computation of the tunnel concentrations. Instead, the slope coefficients, c_1 and c_2, are used to control these values, where c_1 is proportional to the length of the tunnel and c_2 is related to the time it takes for water flowing out of the lake to be only lake water. Figures 6 and 7 depict example solutions for the salinity of water in a tunnel at different times.

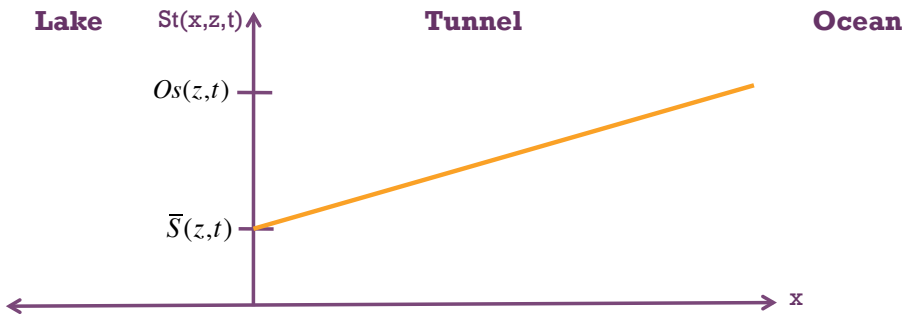

Figure 6: Exact solution to tunnel model for salinity at some time $t = a$.

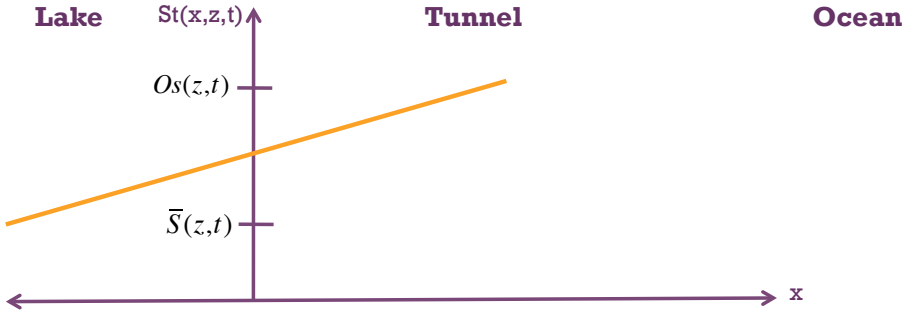

Figure 7: Exact solution to tunnel model for salinity at a later time.

In a later section, we will discuss the methods used to obtain approximations for the velocity of water in the tunnels as well as the slope coefficients.

3 Numerical Methods

To approximate the lake level in equation (1), we use the backward Euler method because it is simple, first order accurate, and A-stable [7]. For each lake concentration model, we apply a combined implicit-explicit numerical scheme. As an example, we focus on deriving a numerical method for approximating the solution to equation (8). We examine the scenarios where water is entering the lake and exiting the lake separately. First we look at the scenario when water is entering the lake, where $\hat{S}(z,t) = Os(z,t)$. We split the right hand side and apply three different methods in conjunction. Since the diffusion component is stiff, we apply the Crank-Nicolson method to allow for larger time step sizes [7]. This method is unconditionally stable and second order accurate in space and time. Discretizing space and time, we let $z = ih$, where $i = 0, 1, ..., I$ and $t = nk$, where $n = 0, 1, ..., N$. Applying Crank-Nicolson to the diffusion component yields:

$$\begin{aligned}\frac{\bar{S}_i^{n+1} - \bar{S}_i^n}{k} = \frac{1}{2A_i}\Bigg[\frac{1}{h}\left(A_{i+\frac{1}{2}}D^n_{i+\frac{1}{2}}\frac{\bar{S}^n_{i+1} - \bar{S}^n_i}{h} - A_{i-\frac{1}{2}}D^n_{i-\frac{1}{2}}\frac{\bar{S}^n_i - \bar{S}^n_{i-1}}{h}\right)\\ +\frac{1}{h}\left(A_{i+\frac{1}{2}}D^{n+1}_{i+\frac{1}{2}}\frac{\bar{S}^{n+1}_{i+1} - \bar{S}^{n+1}_i}{h} - A_{i-\frac{1}{2}}D^{n+1}_{i-\frac{1}{2}}\frac{\bar{S}^{n+1}_i - \bar{S}^{n+1}_{i-1}}{h}\right)\Bigg].\end{aligned}$$

For the $\bar{S}(z,t)$ advection component, we apply the Lax-Wendroff method since it is fairly simple to implement and is also second order accurate in space and time [8]. This method is stable when $k \leq \frac{h}{|u(z)|}$. We approximate $\hat{d}(z)$ using the trapezoidal method to integrate $Tu(z)$ over the appropriate depths. Applying Lax-Wendroff to the $\bar{S}(z,t)$ advection component yields:

$$\begin{aligned}\frac{\bar{S}_i^{n+1} - \bar{S}_i^n}{k} =& -\frac{1}{2h}u_0^n\frac{A_0}{A_i}\left(\hat{d}_{i+1}\bar{S}^n_{i+1} - \hat{d}_{i-1}\bar{S}^n_{i-1}\right)\\ &+\frac{k}{2h^2}\left(u_0^n\frac{A_0}{A_i}\right)^2\left(\hat{d}_{i+1}\bar{S}^n_{i+1} - 2\hat{d}_i\bar{S}^n_i + \hat{d}_{i-1}\bar{S}^n_{i-1}\right).\end{aligned}$$

For the $\hat{S}(z,t)$ advection component and any source or sink term, we apply the trapezoidal method since it is second order accurate and is A-stable [8]:

$$\begin{aligned}\frac{\bar{S}_i^{n+1} - \bar{S}_i^n}{k} =& \frac{1}{2}\frac{A_0}{A_i}\Bigg[u_0^n\left(\frac{\hat{d}_{i+1}\hat{S}^n_{i+1} - \hat{d}_{i-1}\hat{S}^n_{i-1}}{2h} - \hat{d}_i\frac{\hat{S}^n_{i+1} - \hat{S}^n_{i-1}}{2h}\right)\\ &+u_0^{n+1}\left(\frac{\hat{d}_{i+1}\hat{S}^{n+1}_{i+1} - \hat{d}_{i-1}\hat{S}^{n+1}_{i-1}}{2h} - \hat{d}_i\frac{\hat{S}^{n+1}_{i+1} - \hat{S}^{n+1}_{i-1}}{2h}\right)\\ &+cr_i(R^n(Sr^n - \bar{S}^n_i) + R^{n+1}(Sr^{n+1} - \bar{S}^{n+1}_i))\Bigg].\end{aligned}$$

In matrix form, the final numerical scheme for when water is entering the lake is (see appendix for complete derivation):

$$\left[I - \frac{k}{2h^2}A_1(A_2D_1B - A_3D_2C) + \frac{k}{2}A_0A_1C_RR^{n+1}\right]\bar{S}^{n+1}$$
$$= \left[I + \frac{k}{2h^2}A_1(A_2D_3B - A_3D_4C) - \frac{k}{2h}u_0^nA_0A_1E + \frac{k^2}{2h^2}(u_0^nA_0A_1)^2F\right.$$
$$\left. -\frac{k}{2}A_0A_1C_RR^n\right]\bar{S}^n + \frac{k}{4h}A_0A_1\left[u_0^n(E - ZG)\hat{S}^n + u_0^{n+1}(E - ZG)\hat{S}^{n+1} + V\right]$$
$$+ \frac{k}{2}A_0A_1C_R(R^nSr^n + R^{n+1}Sr^{n+1}).$$

Next we will look at the scenario when water is exiting the lake, that is when $\hat{S}(z,t) = \bar{S}(z,t)$. We again apply Crank-Nicolson to the diffusion component, Lax-Wendroff to the advection component, and trapezoidal method to any source/sink term. In matrix form, the final numerical scheme is (see appendix for complete derivation):

$$\left[I - \frac{k}{2h^2}A_1(A_2D_1B - A_3D_2C) + \frac{k}{2}A_0A_1C_RR^{n+1}\right]\bar{S}^{n+1}$$
$$= \left[I + \frac{k}{2h^2}A_1(A_2D_3B - A_3D_4C) - \frac{k}{2h}u_0^nA_0A_1ZM + \frac{k^2}{2h^2}(u_0^nA_0A_1Z)^2H\right.$$
$$\left. -\frac{k}{2}A_0A_1C_RR^n\right]\bar{S}^n + \frac{k}{2}A_0A_1C_R(R^nSr^n + R^{n+1}Sr^{n+1}).$$

Note that all matrices are defined at the end of the appendix.

4 Results

4.1 Lake Level and Tunnel Inflow

We validated both the lake level and tunnel concentration model by matching our approximations with known data [5]. In the lake level model, we obtained the ocean level, density of the ocean, and density of the lake from available data [5] and varied the value of our proportionality constant, ω, to achieve the best fit. In the following plots, we demonstrate the flexibility and accuracy of the lake level model by plotting the model and actual lake level for different values of ω.

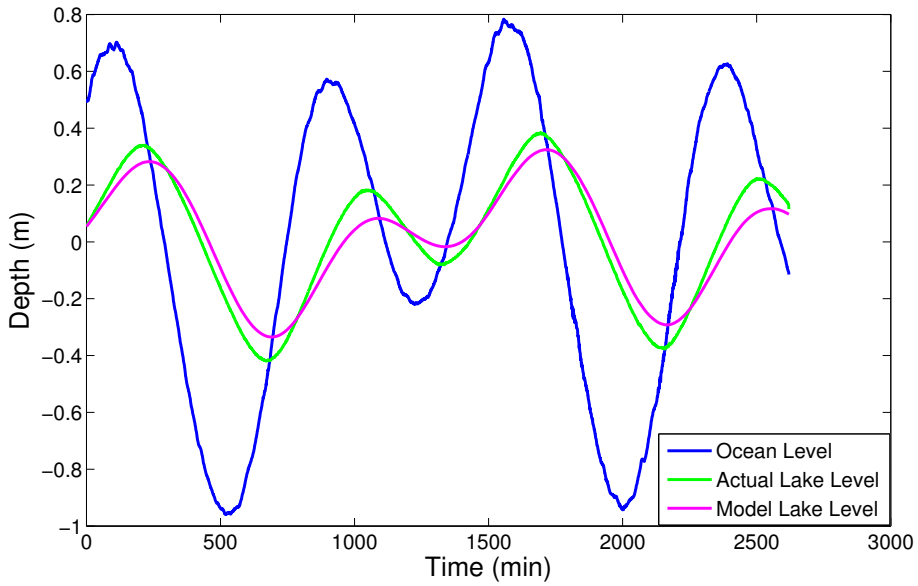

Figure 8: Lake level comparison, where $\omega = 0.0025$. This proportionality constant is too small to match the high or low tide of the lake.

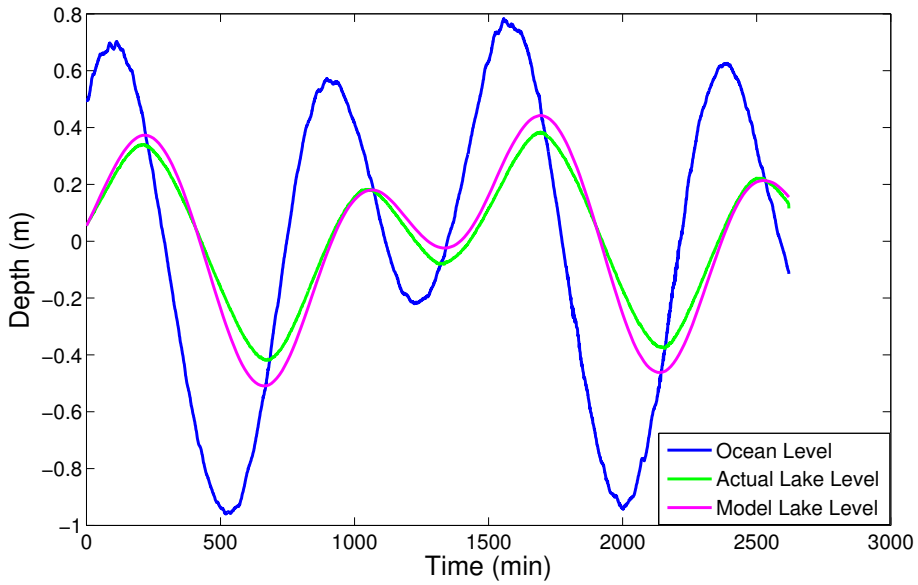

Figure 9: Lake level comparison, where $\omega = 0.0042$. This proportionality constant yields a good match for the low tide peak of the lake, but is too large to match the high tide.

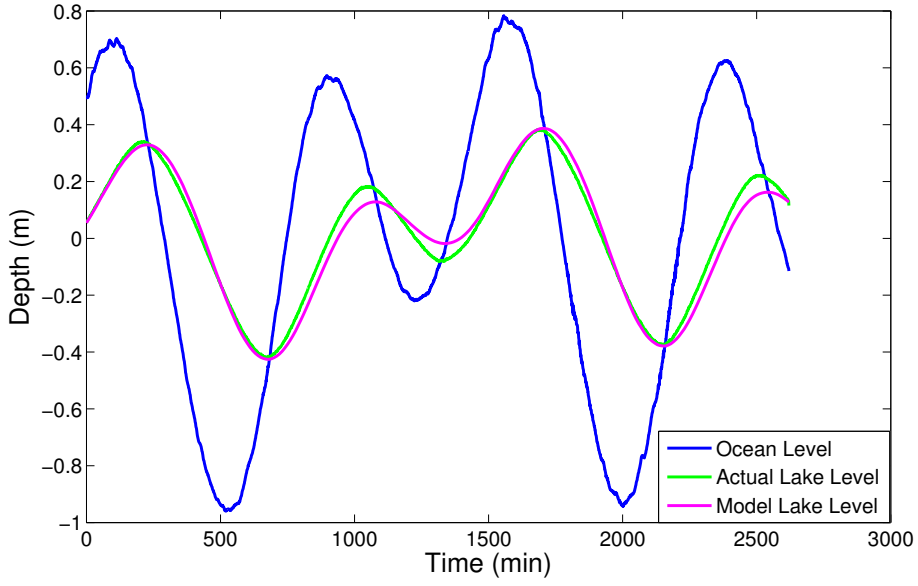

Figure 10: Lake level comparison, where $\omega = 0.0033$. This proportionality constant gave the best fit obtainable with the model. It is unclear why we could not match the low tide of the lake as well as the high tide.

Now that we have validated the lake level model, we examine how well the tunnel inflow model matches the actual data [5]. First we approximate the horizontal velocity of water in the tunnels using the fact that the volume flow rate out of the tunnels or wall of the lake is proportional to the volume flow rate of water in the lake for a given depth:

$$A_{\text{tunnel}}(z)u_{\text{tunnel}}(z,t) \propto u(z,t)A(z),$$
$$u_{\text{tunnel}}(z,t) = \beta(z)\, u(0,t).$$

Here $\beta(z)$ is a dimensionless proportionality constant that is equivalent to

$$\frac{A(0)}{A_{\text{tunnel}}(z)} \int_{-\infty}^{z} T u_{out}(z')dz'.$$

We adjusted the value of $\beta(z)$ to achieve the best fit with the velocity data [5] for a particular tunnel. Since there was only one tunnel for which we had signed velocity data, we used this data to approximate the value of $\beta(z)$ for all tunnels.

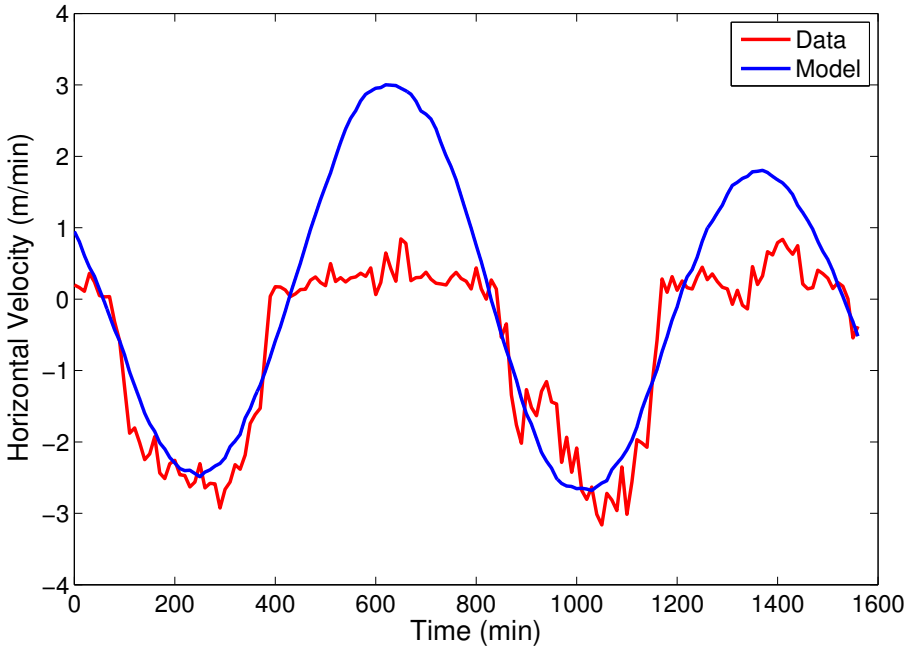

Figure 11: Tunnel (depth $\sim$ 6m) velocity comparison, where $\beta = 1000$. Note that the velocity data does not integrate to zero. This could be due to the sensor being located just outside of the mouth of the tunnel. As a result, the velocity of water flowing out of the tunnel may not be accurately captured.

We chose to best match the tunnel velocity when water is flowing into the lake since this is likely a more accurate representation of the water velocity in the tunnel. When water enters a small opening, its velocity profile is more spread out. This is opposed to when water is exiting a small opening and its velocity profile is more concentrated. So the velocity just outside the opening will be close to that in the tunnel. Moreover, this is when the contents of the tunnel need to be most accurately modeled, as water is flowing into the lake.

Note that although our model provides a good fit for when water is flowing into the lake, the time at which the tide changes from inflow to outflow is delayed by roughly fifty minutes. This could be due to a number of factors. One possibility is that the part of the ocean from which water is flowing into the lake has a different tidal cycle than the ocean data available for that time period. Another factor is the location of the tunnel versus the location of the incoming ocean water.

For all other depths that do not have underground tunnels, we estimated the value of $\beta(z)$ to be ten times smaller than those depths with tunnels. We chose this value because we know that the velocity of water flowing into the lake through the wall of the lake should be significantly less than that through a hollow tunnel. Since we do not have any other data that would provide a more accurate method of approximating it, we made a reasonable guess.

Now that we have a good approximation of the velocity of water in each tunnel, we will compare the salinity and temperature of water at the mouth of a tunnel. We do not compare the oxygen content in the tunnel simply because we do not have any data for it. In the exact solution for the tunnel concentration model, we have two parameters, c_1 and c_2, that we adjust to obtain the best fit.

After shifting the model concentration back by 50 minutes to account for the tidal cycle discrepancy, we obtain a good fit for the salinity of water at the opening of the tunnel, as shown in Figure 12.

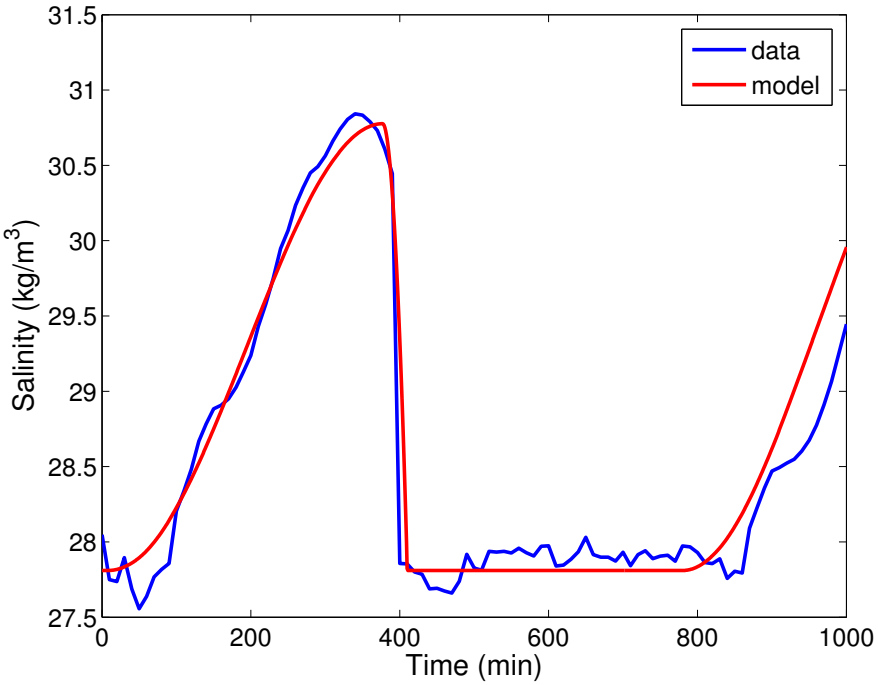

Figure 12: Salinity of water at mouth of tunnel (depth $\sim$ 6m). Salinity of ocean is 33.5 kg/m^3

We chose the salinity of the ocean from the available ocean data at the same depth as the tunnel [5]. Note that the ocean data was collected two years prior to the tunnel velocity and concentration data around the same time of year.

Using the same slope parameter values, we compare the temperature of water at the mouth of the tunnel to the data. We chose the ocean temperature in the same way that we chose the ocean salinity. In Figure 13 we see that the ocean temperature is not nearly low enough to account for the significant decrease in temperature of the tunnel water. This is likely due to cooling effects in the tunnel that are not accounted for in the model. As mentioned before, it is possible that the walls of the tunnel are colder than the water flowing through it. As a result, as water flows from the ocean to the lake, it may lose a substantial amount of heat through the walls of the tunnel. In Figure 14, we determine what ocean temperature yields the best fit to the data. In this way, we can get an idea of how significant these changes in temperature that occur in the tunnel are.

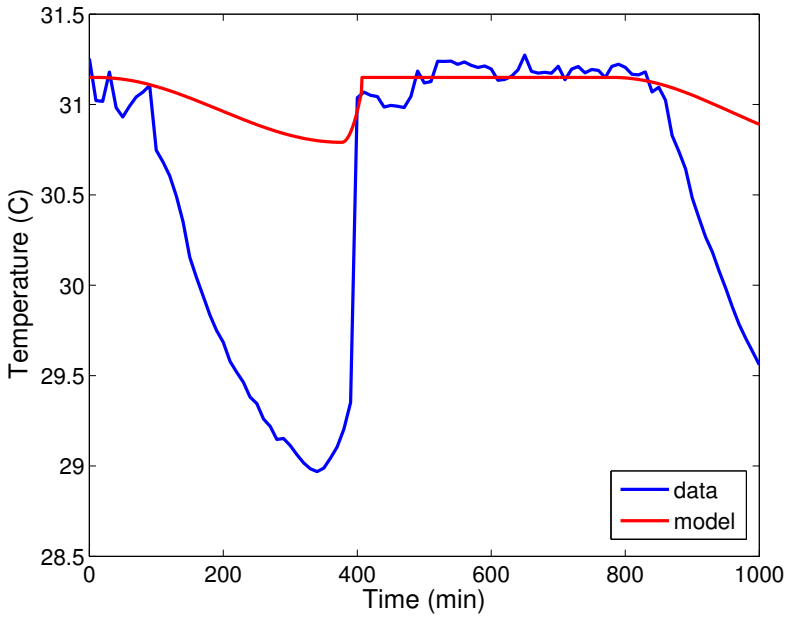

Figure 13: Temperature of water at mouth of tunnel (depth $\sim$ 6m). Temperature of ocean is 30.4°C.

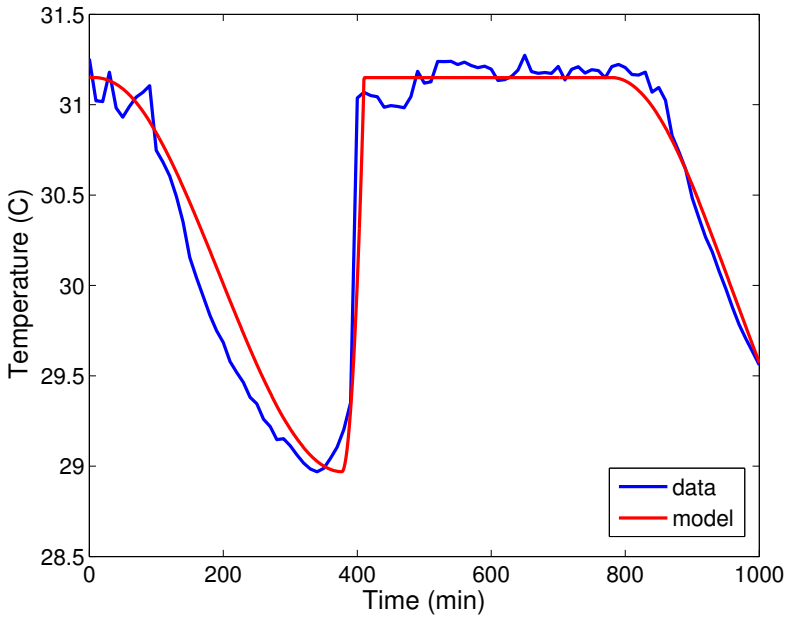

Figure 14: Temperature of water at mouth of tunnel (depth $\sim$ 6m). Temperature of ocean is 26.6°C

We find that there is nearly a 4°C decrease in ocean temperature needed to match the actual tunnel temperature. We can infer from this that choosing $\alpha = 0$ in equation (11) is unrealistic. This is a part of the tunnel model that could be improved upon in the future by determining an appropriate value for α to account for this sink in temperature in the tunnels.

4.2 Stable Lake Simulation

For validation purposes, we will explore how well the lake concentration model does at simulating the lake at equilibrium. Before we begin, we will discuss our choice of diffusion coefficient as well as other parameters and explain the reasoning behind them. We had initially sought to make the diffusion coefficient a function of the lake water density, ρ, and surface wind speed, W, in addition to being a function of depth. Using an appropriate formulation found in [9], we tried the following definition of the diffusion coefficient:

$$D_e(z,t) = \begin{cases} 28W^{1.3} & \text{if} \quad z < z_t \\ 0.00866 D_{\text{max}} N^{-1} & \text{if} \quad z > z_t, \end{cases} \tag{12}$$

where

$$N = \left(\frac{g}{\rho} \frac{\partial \rho}{\partial z} \right)^{1/2}.$$

D_{max} is defined as the maximum diffusion in the hypolimnium, z_t corresponds to the depth of the top of the thermocline, and g is gravitational acceleration. We approximated D_{max} to be the value of diffusion above the thermocline. This formulation did not give us a diffusion profile that we would expect for the lake, since diffusion increased toward the bottom of the lake instead of exhibiting more of an exponential decay. Our next attempt was to combine equation (12) with another formulation found in [10]:

$$D_e(z,t) = e^{-cz} \min(0.00866 D_{\text{max}} N^{-1}\,,\, 28W^{1.3}),$$

where c is the decay constant that we obtained a reasonable approximation for $(1 \cdot 10^{-2}/\text{m})$ from [11]. We chose the minimum between these two values because diffusion in the lake should not exceed the maximum diffusion coefficient as determined by the surface wind speed. This version yielded a diffusion profile that we would expect, however, the order of the diffusion coefficient was too small ($\mathcal{O}(10^{-5})$) to cause any visible diffusive effects. This held true for any realistic wind speed (1-10m/s) for Jellyfish lake [5]. Since this form of the diffusion coefficient yielded negligible values of diffusion for all depths in the lake, we instead chose reasonable values of diffusion for above and below the approximate depth of the pycnocline [5] and made a linear transition between the two values.

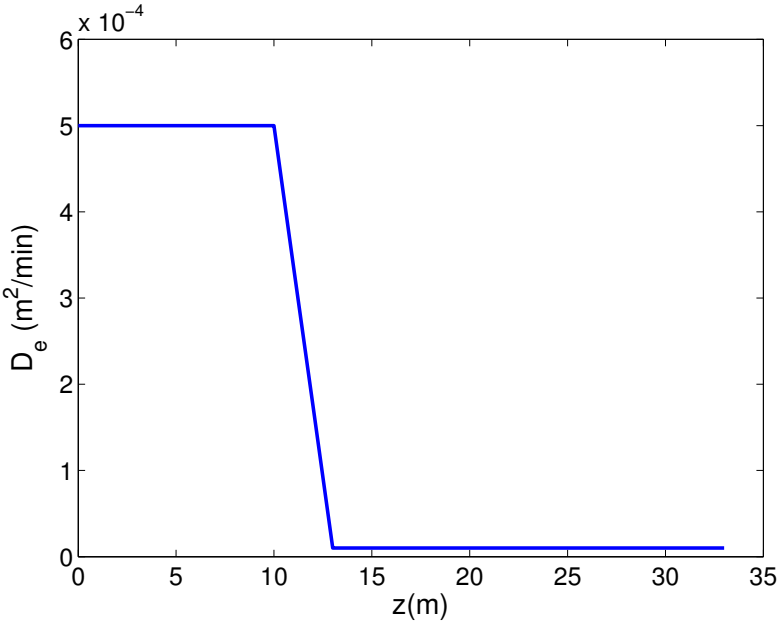

Figure 15: Example choice of diffusion coefficient in lake.

The diffusion coefficient below the pycnocline was chosen to be the largest value that showed no diffusive effects in the lake, while that above the pycnocline was chosen to be the smallest value that showed a reasonable amount of diffusion taking place.

For the remaining parameters in equations (8), (9), and (10) not yet specified, some of these values were obtained from available data while others we made a reasonable guess for due to lack of information. We obtained $A(z)$ as well as the initial conditions for each concentration in the lake from the data [5]. The temperature of the air and rock were assumed to be the temperature of the lake at the surface and the bottom, respectively, since the lake concentrations are supposed to be at equilibrium. The maximum oxygen content in the lake, Ox_{max}, we assumed to be the oxygen content at the surface in the initial condition. For the distribution of inflow and outflow of water in the lake, $Tu(z)$, we chose a high proportion for the depths of known tunnels and evenly distributed the remainder throughout the rest of the lake. For the time being, we set $Sh(z,t)$ and $Oc(z,t)$ to be zero since it was not the primary focus to study the effects of these parameters.

Now to validate the model's ability to simulate a stable lake, we start by comparing a simpler version of the model without modeling flow within the tunnels and the complete version including tunnels. In the simpler version of the model, water flowing into the lake comes directly from the ocean. We approximate the distribution of inflow using a Gaussian function centered near the bottom of the lake, while the distribution of outflow remains the same. Since the salinity of the ocean is known to be greater than any part of the lake from the given data, the salinity of the lake immediately begins increasing and we cannot achieve stable conditions (see Figure 16).

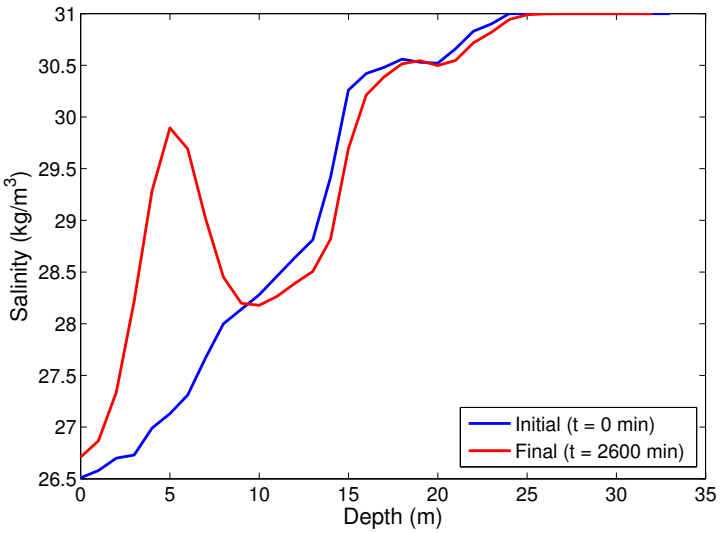

Figure 16: Salinity in lake before tunnels were included in model. The ocean salinity is set to 33.5kg/m^3.

In the complete model, the distribution of inflow is determined by the level of neutral buoyancy of the incoming tunnel water. We assume that the transition time for incoming water to equilibrate with lake water is negligible. To accomplish this, we compute the density of the incoming water at each time step. Then we concurrently determine the distribution of inflow while rearranging the incoming tunnel concentrations according to their level of neutral buoyancy. We determine the level of neutral buoyancy by computing the density of the lake water as a function of salinity and temperature [12]. Using this refined model, we are able to achieve stable lake conditions over time, as can be seen in Figure 17.

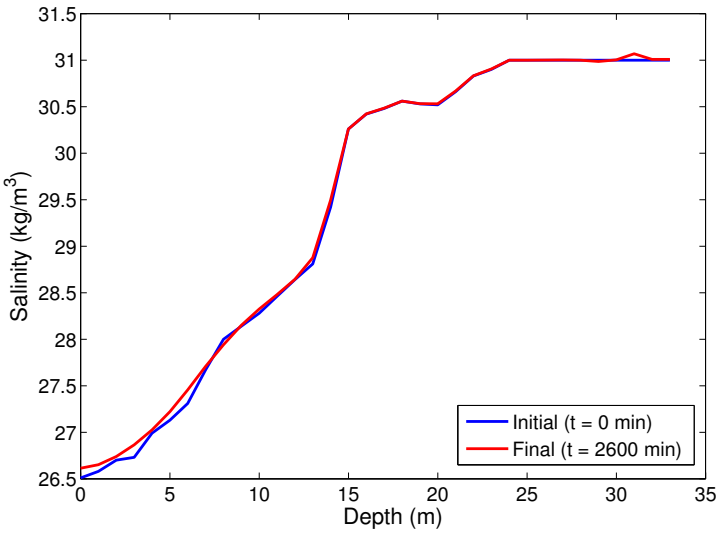

Figure 17: Salinity in lake after tunnels were included in model. The ocean salinity is set to 33.5kg/m^3.

Now that we have confirmed that the model including tunnels can accurately capture stable conditions for salinity in the lake over time, we can plot all three concentrations as a function of depth and time to observe whether conditions are stable for all three concentrations.

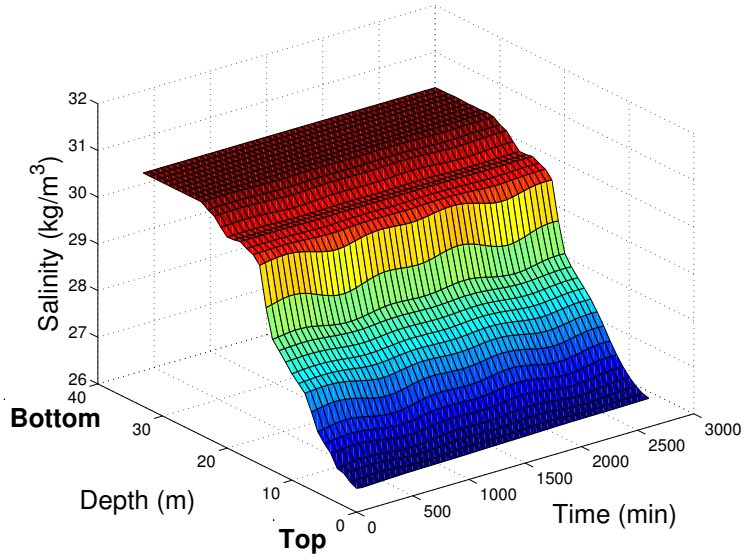

Figure 18: Salinity in lake under stable conditions. The salinity of the ocean is set to 30.25 kg/m^3.

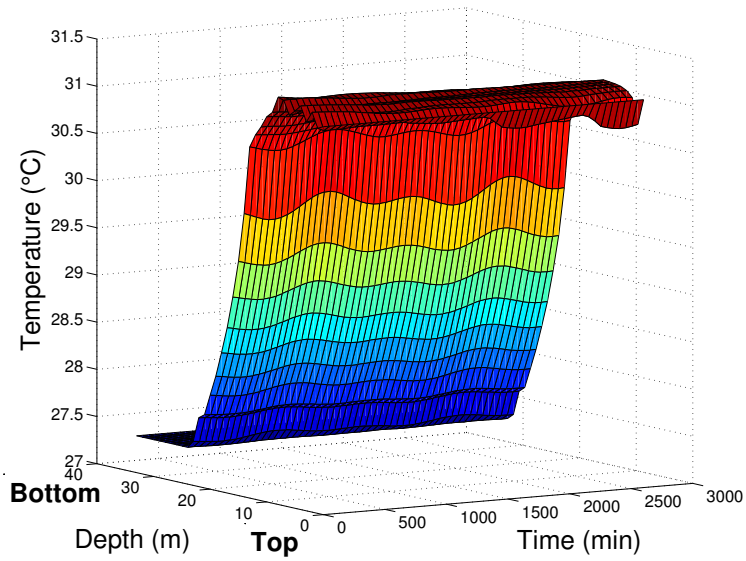

Figure 19: Temperature in lake under stable conditions. The temperature of the ocean is set to 31°C. The temperature of the air and rock are set to value of the initial condition at the top and bottom of the lake, respectively.

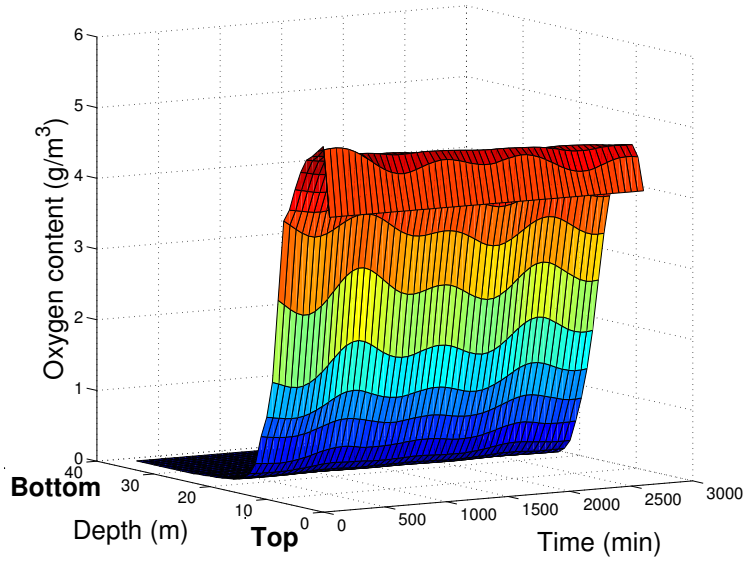

Figure 20: Oxygen in lake under stable conditions. The oxygen content of the ocean is set to 6 $\mathrm{g/m^3}$. The maximum oxygen content of the lake is set to the value of the initial condition at the top of the lake. The oxygen consumption rate is set to $0\mathrm{g/m^3min}$.

From Figures 19 and 20, we see that the lake concentrations indeed remain stable over time.

4.3 Storm Simulation

One of the goals in creating this model is to be able to simulate a tropical storm, where conditions change rapidly. We have been provided with data for the salinity, temperature, and oxygen in the lake before and after a five day storm [5]. After imposing the same initial conditions before the storm, we attempt to match the lake concentration data collected after the storm. Using rainfall data collected during the storm [5], we obtain the average rate of rainfall over that time period, $R = 2.7 \cdot 10^{-5}$m/min. There should be a negligible amount of salt in rainwater so we set Sr to zero. We guess that rainfall should be distributed only in the top meter of the lake so we defined $cr(z)$ accordingly. We do not have any data for the temperature of rainwater so we approximate it using the temperature at the top of the lake after the storm. We also do not have any data for the oxygen content in rainwater, so we approximate it to be the maximum oxygen content in the lake after the storm.

We plot each lake concentration using two different diffusion coefficients in the layer above the pycnocline to demonstrate how the concentration profile changes and the flexibility of the model.

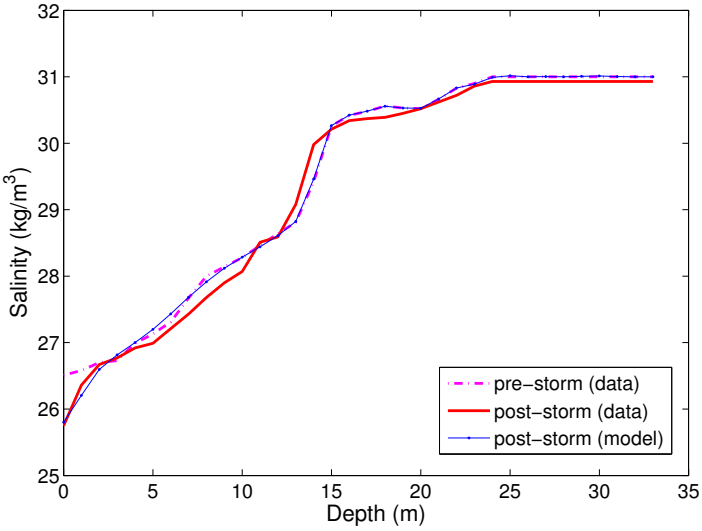

Figure 21: Salinity in lake under storm conditions.

In Figure 21, we observe that after the storm, the salinity profile in the lake remains unchanged except in the top couple of meters, where the salinity decreases. The model was able to capture this change very well after running it for the length of the storm.

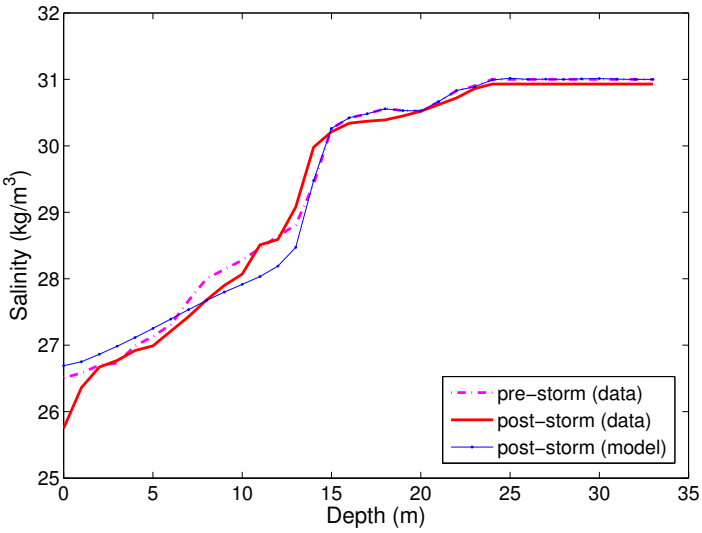

Figure 22: Salinity in lake under storm conditions with high diffusion above the pycnocline.

Figure 22 depicts the effects of making the diffusion coefficient ten times larger above the pycnocline. Although this change does not yield a good fit, we observe that

increasing the diffusion in the model causes more mixing to occur above the pycnocline, as expected.

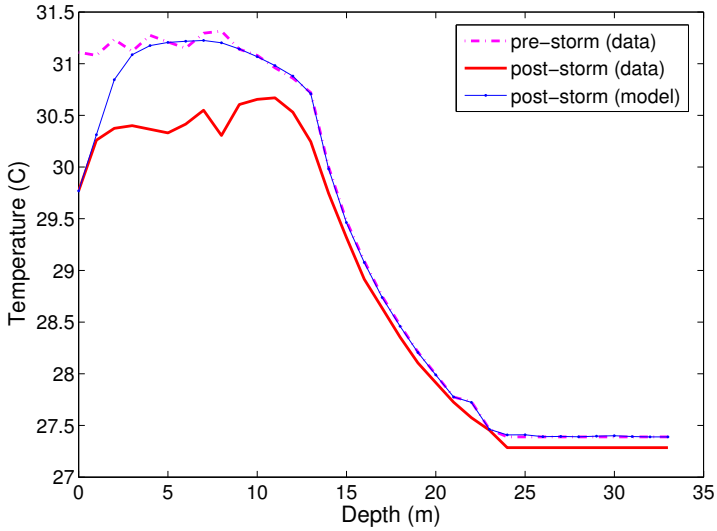

Figure 23: Temperature in lake under storm conditions.

In Figure 23, we observe that the temperature in the lake after the storm decreased significantly in the top 13m. We were not able to obtain a good fit for the temperature profile after the storm. We suspect that this may be due to a number of different factors. One being that the temperature of the rain may be colder than the value that we chose. This is one thing that could be improved upon in the model, potentially by using a Robin boundary condition at the surface that depends on the rate of evaporation and surface wind speed. Another factor is that the model does not take into account any changes in water concentrations flowing into the lake that may be caused by the storm. For instance, the temperature of inflowing water may be colder than usual during a storm. As mentioned before, choosing a nonzero value of α could also change the temperature profile in the lake by considering the change in tunnel water temperature as water flows to and from the ocean.

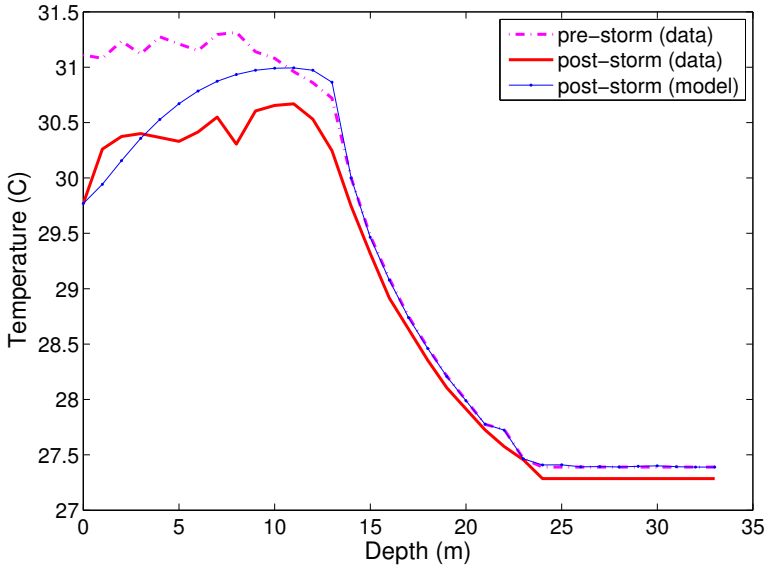

Figure 24: Temperature in lake under storm conditions with high diffusion above the pycnocline.

When using a higher diffusion coefficient for temperature under the same storm conditions, we obtain a slightly better fit to the profile after the storm, as can be seen in Figure 24. However, there is still clearly something else that is not being captured as mentioned before.

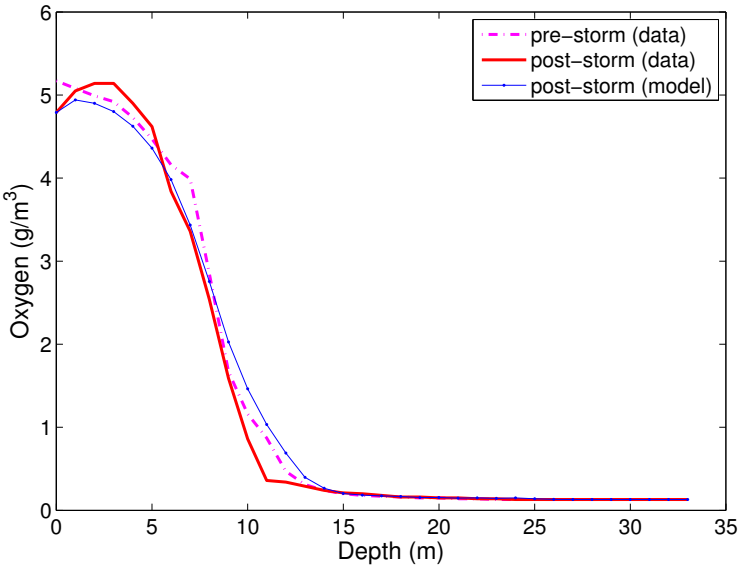

Figure 25: Oxygen in lake under storm conditions. $Oxr = 5.14\text{g/m}^3$.

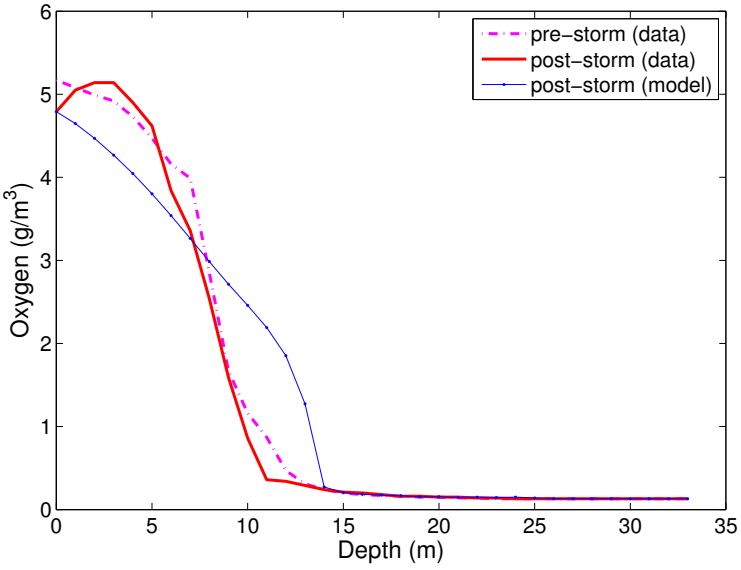

Figure 26: Oxygen in lake under storm conditions with high diffusion above the pycnocline.

In Figure 25, we observe that the oxygen profile in the lake remains relatively unchanged after the storm. The model yielded a decent fit for after the storm. We again take

note of the mixing effects that are caused by a higher diffusion coefficient in the top layer of the lake in Figure 26. Since the oxygen content in the lake was not the primary focus in modeling, we did not explore what the oxygen consumption rate in the lake should be. This as well as the maximum oxygen content in the lake are two topics that could be further explored and improved upon in the future.

5 Conclusion

We have created a model that can simulate the time evolution of the tide level, salinity, temperature, and oxygen in a marine lake, taking into account the concentration of water flowing in from underground tunnels between the ocean and the lake. In addition, we have made the model as flexible as possible by incorporating many different parameters that can be altered for the purpose of exploring the lake's response to various external conditions. Both of these accomplishments have allowed us to accurately simulate the change in salinity profile in Jellyfish lake during a tropical storm.

There are still improvements that can be made to improve the accuracy of the model. As previously mentioned, one component that could be improved upon is the surface boundary conditions for temperature. Instead of using a non-homogeneous Dirichlet boundary condition, a Robin boundary condition involving the evaporation rate and surface wind speed could be implemented. Another area that still has room for improvement is the tunnel concentration model. To better match the horizontal velocity profile in a tunnel, the model could take into account the location of the tunnel versus the part of the ocean that water is flowing to and from. This would better account for any differences in tidal cycle. The tunnel concentration model could also be improved by considering changes in the water temperature that are caused by a difference in temperature of the tunnel walls or by changes occurring during a storm.

This model has a myriad of potential applications. One example is that it could be used to model climate change and by extension, human effects on marine lakes and wildlife. By simply adjusting a few parameters (e.g. increasing solar heat, increasing the amount of annual rainfall, making the ocean warmer and more saline), one could determine whether the resulting temperature profile after some period of time is conducive to the organisms that inhabit the lake. It could also be used to model natural mixing, like that due to the existence of large populations of golden jellyfish. Since these jellyfish migrate to different depths of the lake depending on the time of day [5], the diffusion coefficient could be written to encompass this effect. One could then conceivably determine whether the lake would remain stratified or become well-mixed over time. The answer to this question is paramount because it can be a determining factor to the survival of lake ecosystems. Yet another possible application of this model is to study the effect that drastic weather variations, like El Niño, have on marine lakes and their ecosystems. The model could be run for the projected period of El Niño to determine whether there is a threshold time at which lake conditions are no longer inhabitable for the existing plants and organisms. In creating this model, we have made something that is practical to use and flexible in its applicability, with the intention that it can be utilized by U.C. Merced's Quantitative and Systems Biology department for future studies.

6 Appendix

Numerical derivation of salinity equation during inflow:

Putting the three methods together into one numerical scheme yields:

$$\begin{aligned}
\frac{\bar{S}_i^{n+1}-\bar{S}_i^n}{k} &= \frac{1}{2A_i}\left[\frac{1}{h}\left(A_{i+\frac{1}{2}}D^n_{i+\frac{1}{2}}\frac{\bar{S}^n_{i+1}-\bar{S}^n_i}{h}-A_{i-\frac{1}{2}}D^n_{i-\frac{1}{2}}\frac{\bar{S}^n_i-\bar{S}^n_{i-1}}{h}\right)\right.\\
&\quad\left.+\frac{1}{h}\left(A_{i+\frac{1}{2}}D^{n+1}_{i+\frac{1}{2}}\frac{\bar{S}^{n+1}_{i+1}-\bar{S}^{n+1}_i}{h}-A_{i-\frac{1}{2}}D^{n+1}_{i-\frac{1}{2}}\frac{\bar{S}^{n+1}_i-\bar{S}^{n+1}_{i-1}}{h}\right)\right]\\
&\quad-\frac{1}{2h}u_0^n\frac{A_0}{A_i}\left[(\hat{d}_{i+1}\bar{S}^n_{i+1}-\hat{d}_{i-1}\bar{S}^n_{i-1})\right]+\frac{k}{2h^2}\left(u_0^n\frac{A_0}{A_i}\right)^2\left[(\hat{d}_{i+1}\bar{S}^n_{i+1}-2\hat{d}_i\bar{S}^n_i+\hat{d}_{i-1}\bar{S}^n_{i-1})\right]\\
&\quad+\frac{1}{2}\frac{A_0}{A_i}\left[u_0^n\left(\frac{\hat{d}_{i+1}\hat{S}^n_{i+1}-\hat{d}_{i-1}\hat{S}^n_{i-1}}{2h}-\hat{d}_i\frac{\hat{S}^n_{i+1}-\hat{S}^n_{i-1}}{2h}\right)\right.\\
&\quad\left.+u_0^{n+1}\left(\frac{\hat{d}_{i+1}\hat{S}^{n+1}_{i+1}-\hat{d}_{i-1}\hat{S}^{n+1}_{i-1}}{2h}-\hat{d}_i\frac{\hat{S}^{n+1}_{i+1}-\hat{S}^{n+1}_{i-1}}{2h}\right)\right.\\
&\quad\left.+cr_i(R^n(Sr^n-\bar{S}^n_i)+R^{n+1}(Sr^{n+1}-\bar{S}^{n+1}_i))\right],
\end{aligned}$$

$$\begin{aligned}
&\bar{S}_i^{n+1}-\frac{k}{2h^2}\frac{1}{A_i}\left(A_{i+\frac{1}{2}}D^{n+1}_{i+\frac{1}{2}}(\bar{S}^{n+1}_{i+1}-\bar{S}^{n+1}_i)-A_{i-\frac{1}{2}}D^{n+1}_{i-\frac{1}{2}}(\bar{S}^{n+1}_i-\bar{S}^{n+1}_{i-1})\right)\\
&+\frac{k}{2}\frac{A_0}{A_i}cr_iR^{n+1}\bar{S}^{n+1}_i=\bar{S}^n_i+\frac{k}{2h^2}\frac{1}{A_i}\left(A_{i+\frac{1}{2}}D^n_{i+\frac{1}{2}}(\bar{S}^n_{i+1}-\bar{S}^n_i)-A_{i-\frac{1}{2}}D^n_{i-\frac{1}{2}}(\bar{S}^n_i-\bar{S}^n_{i-1})\right)\\
&\quad-\frac{k}{2h}u_0^n\frac{A_0}{A_i}(\hat{d}_{i+1}\bar{S}^n_{i+1}-\hat{d}_{i-1}\bar{S}^n_{i-1})+\frac{k^2}{2h^2}\left(u_0^n\frac{A_0}{A_i}\right)^2(\hat{d}_{i+1}\bar{S}^n_{i+1}-2\hat{d}_i\bar{S}^n_i+\hat{d}_{i-1}\bar{S}^n_{i-1})\\
&\quad-\frac{k}{2}\frac{A_0}{A_i}cr_iR^n\bar{S}^n_i+\frac{k}{4h}\frac{A_0}{A_i}\left[u_0^n\left(\hat{d}_{i+1}\hat{S}^n_{i+1}-\hat{d}_{i-1}\hat{S}^n_{i-1}-\hat{d}_i(\hat{S}^n_{i+1}-\hat{S}^n_{i-1})\right)\right.\\
&\left.+u_0^{n+1}\left(\hat{d}_{i+1}\hat{S}^{n+1}_{i+1}-\hat{d}_{i-1}\hat{S}^{n+1}_{i-1}-\hat{d}_i(\hat{S}^{n+1}_{i+1}-\hat{S}^{n+1}_{i-1})\right)\right]+\frac{k}{2}\frac{A_0}{A_i}cr_i(R^nSr^n+R^{n+1}Sr^{n+1}),
\end{aligned}$$

$$\begin{aligned}
&\left[I-\frac{k}{2h^2}A_1(A_2D_1B-A_3D_2C)+\frac{k}{2}A_0A_1C_RR^{n+1}\right]\bar{S}^{n+1}\\
&\quad=\left[I+\frac{k}{2h^2}A_1(A_2D_3B-A_3D_4C)-\frac{k}{2h}u_0^nA_0A_1E+\frac{k^2}{2h^2}(u_0^nA_0A_1)^2F\right.\\
&\quad\left.-\frac{k}{2}A_0A_1C_RR^n\right]\bar{S}^n+\frac{k}{4h}A_0A_1\left[u_0^n(E-ZG)\hat{S}^n+u_0^{n+1}(E-ZG)\hat{S}^{n+1}+V\right]\\
&\quad+\frac{k}{2}A_0A_1C_R(R^nSr^n+R^{n+1}Sr^{n+1}).
\end{aligned}$$

Applying the previously found boundary condition to the numerical scheme at $i = 0$, we obtain

$$\begin{aligned}
&\bar{S}_0^{n+1} - \frac{k}{2h^2}\frac{1}{A_0}\left(A_{\frac{1}{2}}D_{\frac{1}{2}}^{n+1}(\bar{S}_1^{n+1} - \bar{S}_0^{n+1}) - A_{-\frac{1}{2}}D_{-\frac{1}{2}}^{n+1}(\bar{S}_0^{n+1} - \bar{S}_1^{n+1})\right) \\
&\quad + \frac{k}{2}cr_0R^{n+1}\bar{S}_0^{n+1} = \bar{S}_0^n + \frac{k}{2h^2}\frac{1}{A_0}\left(A_{\frac{1}{2}}D_{\frac{1}{2}}^{n}(\bar{S}_1^{n} - \bar{S}_0^{n}) - A_{-\frac{1}{2}}D_{-\frac{1}{2}}^{n}(\bar{S}_0^{n} - \bar{S}_1^{n})\right) \\
&\qquad - \frac{k}{2h}u_0^n(\hat{d}_1 - \hat{d}_{-1})\bar{S}_1^n + \frac{k^2}{2h^2}\left(u_0^n\right)^2\left((\hat{d}_1 + \hat{d}_{-1})\bar{S}_1^n - 2\hat{d}_0\bar{S}_0^n\right) \\
&\qquad - \frac{k}{2}cr_0R^n\bar{S}_0^n + \frac{k}{4h}\left[u_0^n\left(\hat{d}_1 - \hat{d}_0\right)\hat{S}_1^n + u_0^{n+1}\left(\hat{d}_1 - \hat{d}_0\right)\hat{S}_1^{n+1}\right] \\
&\quad + \frac{k}{4h}\left[u_0^n(-\hat{d}_{-1} + \hat{d}_0)\hat{S}_{-1}^n + u_0^{n+1}(-\hat{d}_{-1} + \hat{d}_0)\hat{S}_{-1}^{n+1}\right] + \frac{k}{2}cr_0(R^nSr^n + R^{n+1}Sr^{n+1}).
\end{aligned}$$

Similarly, at $i = I$, we obtain

$$\begin{aligned}
&\bar{S}_I^{n+1} - \frac{k}{2h^2}\frac{1}{A_I}\left(A_{I+\frac{1}{2}}D_{I+\frac{1}{2}}^{n+1}(\bar{S}_{I-1}^{n+1} - \bar{S}_I^{n+1}) - A_{I-\frac{1}{2}}D_{I-\frac{1}{2}}^{n+1}(\bar{S}_I^{n+1} - \bar{S}_{I-1}^{n+1})\right) \\
&\qquad + \frac{k}{2}\frac{A_0}{A_I}cr_IR^{n+1}\bar{S}_I^{n+1} \\
&\quad = \bar{S}_I^n + \frac{k}{2h^2}\frac{1}{A_I}\left(A_{I+\frac{1}{2}}D_{I+\frac{1}{2}}^{n}(\bar{S}_{I-1}^{n} - \bar{S}_I^{n}) - A_{I-\frac{1}{2}}D_{I-\frac{1}{2}}^{n}(\bar{S}_I^{n} - \bar{S}_{I-1}^{n})\right) \\
&\qquad - \frac{k}{2h}u_0^n\frac{A_0}{A_I}(\hat{d}_{I+1} - \hat{d}_{I-1})\bar{S}_{I-1}^n + \frac{k^2}{2h^2}\left(u_0^n\frac{A_0}{A_I}\right)^2\left((\hat{d}_{I+1} + \hat{d}_{I-1})\bar{S}_{I-1}^n - 2\hat{d}_I\bar{S}_I^n\right) \\
&\qquad - \frac{k}{2}\frac{A_0}{A_I}cr_IR^n\bar{S}_I^n + \frac{k}{4h}\frac{A_0}{A_I}\left[u_0^n\left(-\hat{d}_{I-1} + \hat{d}_I\right)\hat{S}_{I-1}^n + u_0^{n+1}\left(-\hat{d}_{I-1} + \hat{d}_I\right)\hat{S}_{I-1}^{n+1}\right] \\
&\qquad + \frac{k}{4h}\frac{A_0}{A_I}\left[u_0^n(\hat{d}_{I+1} - \hat{d}_I)\hat{S}_{I+1}^n + (\hat{d}_{I+1} - \hat{d}_I)\hat{S}_{I+1}^{n+1}\right] \\
&\qquad + \frac{k}{2}\frac{A_0}{A_I}cr_I(R^nSr^n + R^{n+1}Sr^{n+1}).
\end{aligned}$$

Numerical derivation of salinity equation during outflow:

Putting the three methods together into one numerical scheme yields:

$$\begin{aligned}\frac{\bar{S}_i^{n+1}-\bar{S}_i^n}{k} &= \frac{1}{2A_i}\left[\frac{1}{h}\left(A_{i+\frac{1}{2}}D^n_{i+\frac{1}{2}}\frac{\bar{S}^n_{i+1}-\bar{S}^n_i}{h}-A_{i-\frac{1}{2}}D^n_{i-\frac{1}{2}}\frac{\bar{S}^n_i-\bar{S}^n_{i-1}}{h}\right)\right.\\ &\quad\left.+\frac{1}{h}\left(A_{i+\frac{1}{2}}D^{n+1}_{i+\frac{1}{2}}\frac{\bar{S}^{n+1}_{i+1}-\bar{S}^{n+1}_i}{h}-A_{i-\frac{1}{2}}D^{n+1}_{i-\frac{1}{2}}\frac{\bar{S}^{n+1}_i-\bar{S}^{n+1}_{i-1}}{h}\right)\right]\\ &\quad-\frac{1}{2h}u_0^n\frac{A_0}{A_i}\hat{d}_i(\bar{S}^n_{i+1}-\bar{S}^n_{i-1})+\frac{k}{2h^2}\left(u_0^n\frac{A_0}{A_i}\hat{d}_i\right)^2(\bar{S}^n_{i+1}-2\bar{S}^n_i+\bar{S}^n_{i-1})\\ &\quad+\frac{1}{2}\frac{A_0}{A_i}cr_i(R^n(Sr^n-\bar{S}^n_i)+R^{n+1}(Sr^{n+1}-\bar{S}^{n+1}_i)),\end{aligned}$$

$$\begin{aligned}&\bar{S}_i^{n+1}-\frac{k}{2h^2}\frac{1}{A_i}\left(A_{i+\frac{1}{2}}D^{n+1}_{i+\frac{1}{2}}(\bar{S}^{n+1}_{i+1}-\bar{S}^{n+1}_i)-A_{i-\frac{1}{2}}D^{n+1}_{i-\frac{1}{2}}(\bar{S}^{n+1}_i-\bar{S}^{n+1}_{i-1})\right)\\ &\qquad+\frac{k}{2}\frac{A_0}{A_i}cr_iR^{n+1}\bar{S}^{n+1}_i\\ &=\bar{S}^n_i+\frac{k}{2h^2}\frac{1}{A_i}\left(A_{i+\frac{1}{2}}D^n_{i+\frac{1}{2}}(\bar{S}^n_{i+1}-\bar{S}^n_i)-A_{i-\frac{1}{2}}D^n_{i-\frac{1}{2}}(\bar{S}^n_i-\bar{S}^n_{i-1})\right)\\ &\quad-\frac{k}{2h}u_0^n\frac{A_0}{A_i}\hat{d}_i(\bar{S}^n_{i+1}-\bar{S}^n_{i-1})+\frac{k^2}{2h^2}\left(u_0^n\frac{A_0}{A_i}\hat{d}_i\right)^2(\bar{S}^n_{i+1}-2\bar{S}^n_i+\bar{S}^n_{i-1})\\ &\qquad-\frac{k}{2}\frac{A_0}{A_i}cr_iR^n\bar{S}^n_i+\frac{k}{2}\frac{A_0}{A_i}cr_i(R^nSr^n+R^{n+1}Sr^{n+1}),\end{aligned}$$

$$\begin{aligned}&\left[I-\frac{k}{2h^2}A_1(A_2D_1B-A_3D_2C)+\frac{k}{2}A_0A_1C_RR^{n+1}\right]\bar{S}^{n+1}\\ &\quad=\left[I+\frac{k}{2h^2}A_1(A_2D_3B-A_3D_4C)-\frac{k}{2h}u_0^nA_0A_1ZM+\frac{k^2}{2h^2}(u_0^nA_0A_1Z)^2H\right.\\ &\qquad\left.-\frac{k}{2}A_0A_1C_RR^n\right]\bar{S}^n+\frac{k}{2}A_0A_1C_R(R^nSr^n+R^{n+1}Sr^{n+1}).\end{aligned}$$

Applying the previously found boundary condition to our numerical scheme at $i = 0$, we obtain

$$\bar{S}_0^{n+1} - \frac{k}{2h^2}\frac{1}{A_0}\left(A_{\frac{1}{2}}D_{\frac{1}{2}}^{n+1}(\bar{S}_1^{n+1} - \bar{S}_0^{n+1}) - A_{-\frac{1}{2}}D_{-\frac{1}{2}}^{n+1}(\bar{S}_0^{n+1} - \bar{S}_1^{n+1})\right)$$
$$+ \frac{k}{2}cr_0R^{n+1}\bar{S}_0^{n+1} = \bar{S}_0^n + \frac{k}{2h^2}\frac{1}{A_0}\left(A_{\frac{1}{2}}D_{\frac{1}{2}}^{n}(\bar{S}_1^{n} - \bar{S}_0^{n}) - A_{-\frac{1}{2}}D_{-\frac{1}{2}}^{n}(\bar{S}_0^{n} - \bar{S}_1^{n})\right)$$
$$+ \frac{k^2}{2h^2}\left(u_0^n\hat{d}_0\right)^2(2\bar{S}_1^n - 2\bar{S}_0^n) - \frac{k}{2}cr_0R^n\bar{S}_0^n + \frac{k}{2}cr_0(R^nSr^n + R^{n+1}Sr^{n+1}).$$

Similarly, at $i = I$, we obtain

$$\bar{S}_I^{n+1} - \frac{k}{2h^2}\frac{1}{A_I}\left(A_{I+\frac{1}{2}}D_{I+\frac{1}{2}}^{n+1}(\bar{S}_{I-1}^{n+1} - \bar{S}_I^{n+1}) - A_{I-\frac{1}{2}}D_{I-\frac{1}{2}}^{n+1}(\bar{S}_I^{n+1} - \bar{S}_{I-1}^{n+1})\right)$$
$$+ \frac{k}{2}\frac{A_0}{A_I}cr_IR^{n+1}\bar{S}_I^{n+1}$$
$$= \bar{S}_I^n + \frac{k}{2h^2}\frac{1}{A_I}\left(A_{I+\frac{1}{2}}D_{I+\frac{1}{2}}^{n}(\bar{S}_{I-1}^{n} - \bar{S}_I^{n}) - A_{I-\frac{1}{2}}D_{I-\frac{1}{2}}^{n}(\bar{S}_I^{n} - \bar{S}_{I-1}^{n})\right)$$
$$+ \frac{k^2}{2h^2}\left(u_0^n\frac{A_0}{A_I}\hat{d}_I\right)^2(2\bar{S}_{I-1}^n - 2\bar{S}_I^n) - \frac{k}{2}\frac{A_0}{A_I}cr_IR^n\bar{S}_I^n + \frac{k}{2}\frac{A_0}{A_I}cr_I(R^nSr^n + R^{n+1}Sr^{n+1}).$$

Matrix Definitions

The differentiation and coefficient matrices are defined as follows:

$$A_1 = \begin{bmatrix} \frac{1}{A(z_0)} & & & \\ & \frac{1}{A(z_1)} & & \\ & & \ddots & \\ & & & \frac{1}{A(z_I)} \end{bmatrix}$$

$$A_2 = \begin{bmatrix} A(z_{\frac{1}{2}}) & & & \\ & A(z_{\frac{3}{2}}) & & \\ & & \ddots & \\ & & & A(z_{I+\frac{1}{2}}) \end{bmatrix}$$

$$A_3 = \begin{bmatrix} A(z_{-\frac{1}{2}}) & & & \\ & A(z_{\frac{1}{2}}) & & \\ & & \ddots & \\ & & & A(z_{I-\frac{1}{2}}) \end{bmatrix}$$

$$B = \begin{bmatrix} -1 & 1 & & & \\ & -1 & 1 & & \\ & & \ddots & \ddots & \\ & & & -1 & 1 \\ & & & 1 & -1 \end{bmatrix}$$

$$C = \begin{bmatrix} 1 & -1 & & & \\ -1 & 1 & & & \\ & \ddots & \ddots & & \\ & & -1 & 1 & \\ & & & -1 & 1 \end{bmatrix}$$

$$C_R = \begin{bmatrix} cr_0 & & & \\ & cr_1 & & \\ & & \ddots & \\ & & & cr_I \end{bmatrix}$$

$$D_1 = \begin{bmatrix} D(z_{\frac{1}{2}}, t^{n+1}) & & & \\ & D(z_{\frac{3}{2}}, t^{n+1}) & & \\ & & \ddots & \\ & & & D(z_{I+\frac{1}{2}}, t^{n+1}) \end{bmatrix}$$

$$D_2 = \begin{bmatrix} D(z_{-\frac{1}{2}}, t^{n+1}) & & & \\ & D(z_{\frac{1}{2}}, t^{n+1}) & & \\ & & \ddots & \\ & & & D(z_{I-\frac{1}{2}}, t^{n+1}) \end{bmatrix}$$

$$D_3 = \begin{bmatrix} D(z_{\frac{1}{2}}, t^{n}) & & & \\ & D(z_{\frac{3}{2}}, t^{n}) & & \\ & & \ddots & \\ & & & D(z_{I+\frac{1}{2}}, t^{n}) \end{bmatrix}$$

$$D_4 = \begin{bmatrix} D(z_{-\frac{1}{2}}, t^{n}) & & & \\ & D(z_{\frac{1}{2}}, t^{n}) & & \\ & & \ddots & \\ & & & D(z_{I-\frac{1}{2}}, t^{n}) \end{bmatrix}$$

$$E = \begin{bmatrix} 0 & \hat{d}_1 - \hat{d}_{-1} & & & \\ -\hat{d}_0 & 0 & \hat{d}_2 & & \\ & \ddots & \ddots & \ddots & \\ & & -\hat{d}_{I-2} & 0 & \hat{d}_I \\ & & & \hat{d}_{I+1} - \hat{d}_{I-1} & 0 \end{bmatrix}$$

$$F = \begin{bmatrix} -2\hat{d}_0 & \hat{d}_1 + \hat{d}_{-1} & & & \\ \hat{d}_0 & -2\hat{d}_1 & \hat{d}_2 & & \\ & \ddots & \ddots & \ddots & \\ & & \hat{d}_{I-2} & -2\hat{d}_{I-1} & \hat{d}_I \\ & & & \hat{d}_{I+1} + \hat{d}_{I-1} & -2\hat{d}_I \end{bmatrix}$$

$$G = \begin{bmatrix} 0 & 1 & & & \\ -1 & 0 & 1 & & \\ & \ddots & \ddots & \ddots & \\ & & -1 & 0 & 1 \\ & & & -1 & 0 \end{bmatrix}$$

$$H = \begin{bmatrix} -2 & 2 & & & \\ 1 & -2 & 1 & & \\ & \ddots & \ddots & \ddots & \\ & & 1 & -2 & 1 \\ & & & 2 & -2 \end{bmatrix}$$

$$M = \begin{bmatrix} 0 & 0 & & & \\ -1 & 0 & 1 & & \\ & \ddots & \ddots & \ddots & \\ & & -1 & 0 & 1 \\ & & & 0 & 0 \end{bmatrix}$$

$$V = \begin{bmatrix} \frac{k}{4h}\left[u_0^n(-\hat{d}_{-1}+\hat{d}_0)\hat{S}_{-1}^n + u_0^{n+1}(-\hat{d}_{-1}+\hat{d}_0)\hat{S}_{-1}^{n+1}\right] \\ 0 \\ \vdots \\ 0 \\ \frac{k}{4h}\frac{A_0}{A_I}\left[u_0^n(\hat{d}_{I+1}-\hat{d}_I)\hat{S}_{I+1}^n + (\hat{d}_{I+1}-\hat{d}_I)\hat{S}_{I+1}^{n+1}\right] \end{bmatrix}$$

$$Z = \begin{bmatrix} \hat{d}_0 & & & \\ & \hat{d}_1 & & \\ & & \ddots & \\ & & & \hat{d}_I \end{bmatrix}$$

7 References

[1] Hamner, W.M. and P.P. Hamner, *Stratified marine lakes of Palau (Western Caroline Islands)*, Physical Geography, 19 : 175-220 (1998)

[2] Vincent, W.F. and Likens, G.E. *Encyclopedia of Inland Waters*. Oxford: Academic Press, 2009. ScienceDirect. Web. 5 Aug. 2013.

[3] Katija, K. and Dabiri, J.O., *A viscosity-enhanced mechanism for biogenic ocean mixing*, Nature, 460 : 624-626 (2009)

[4] Martin et al., *Marine lake ecosystem dynamics illustrate ENSO variation in the tropical western Pacific*, Biol. Lett., 2 : 144-147 (2006)

[5] Dawson, Mike. Personal communication. Mar. 2012 - Aug. 2013.

[6] Linacre, E.T., *A simple formula for estimating evaporation rates in various climates, using temperature data alone*, Agricultural Meteorology, 18 : 409-424 (1977)

[7] Burden, R.L. and Faire, J.D. *Numerical Analysis*. Belmont: Bob Pirtle, 2005. Print.

[8] LeVeque, R.J. *Finite difference methods for ordinary and partial differential equations*. Philadelphia: Society for Industrial and Applied Mathematics, 2007. Print.

[9] Riley, M.J. and Stefan, H.G., *Minlake: A dynamic lake water quality simulation model*, Ecological Modeling, 43 : 155-182 (1988)

[10] Kaufman, P., Grotzinger, J.P., and McCormick, D.S., *Depth-dependent diffusion algorithm for simulation of sedimentation in shallow marine depositional systems*, Kansas Geological Survey, 233 : 489-508 (1991)

[11] Botte, V. and Kay, A., *A model of wind-driven circulation in Lake Baikal*, Dynamics of Atmospheres and Oceans, 35 : 131-152 (2002)

[12] Millero, F.J. and Poisson A., *International one-atmosphere equation of state of seawater*, Deep Sea Research, 28A : 625-629 (1981)